JACS
JOURNAL OF THE AMERICAN CHEMICAL SOCIETY

Article

pubs.acs.org/JACS

Two-Photon Absorbing Phosphorescent Metalloporphyrins: Effects of π-Extension and Peripheral Substitution

Tatiana V. Esipova,[†] Héctor J. Rivera-Jacquez,[§] Bruno Weber,[∥] Artëm E. Masunov,[§,⊥,#,7] and Sergei A. Vinogradov*[,†,‡]

[†]Department of Biochemistry and Biophysics, Perelman School of Medicine, and [‡]Department of Chemistry, School of Arts and Sciences, University of Pennsylvania, Philadelphia, Pennsylvania 19104, United States

[§]NanoScience Technology Center, Department of Chemistry and Department of Physics, University of Central Florida, Orlando, Florida 32816, United States

[∥]Institute of Pharmacology and Toxicology, University of Zurich, Zurich CH-8057, Switzerland

[⊥]Photochemistry Center, Russian Academy of Sciences, ul. Novatorov 7a, Moscow 119421, Russia

[#]South Ural State University, Lenin pr. 76, Chelyabinsk 454080, Russia

[7]National Nuclear Research University MEPhI, Kashirskoye sh. 31, Moscow 115409, Russia

Supporting Information

ABSTRACT: The ability to form triplet excited states upon two-photon excitation is important for several applications of metalloporphyrins, including two-photon phosphorescence lifetime microscopy (2PLM) and two-photon photodynamic therapy (PDT). Here we analyzed one-photon (1P) and degenerate two-photon (2P) absorption properties of several phosphorescent Pt (II) porphyrins, focusing on the effects of aromatic π-extension and peripheral substitution on triplet emissivity and two-photon absorption (2PA). Our 2PA measurements for the first time made use of direct time-resolved detection of phosphorescence, having the ability to efficiently reject laser background through microsecond time gating. π-Extension of the porphyrin macrocycle by way of *syn*-fusion with two external aromatic fragments, such as in *syn*-dibenzo- (DBP) and *syn*-dinaphthoporphyrins (DNP), lowers the symmetry of the porphyrin skeleton. As a result, DBPs and DNPs exhibit stronger 2PA into the one-photon-allowed B (Soret) and Q states than fully symmetric (D_{4h}) nonextended porphyrins. However, much more 2P-active states lie above the B state and cannot be accessed due to the interfering linear absorption. Alkoxycarbonyl groups (CO_2R) in the benzo-rings dramatically enhance 2PA near the B state level. Time-dependent density functional theory (TDDFT) calculations in combinations with the sum-over-states (SOS) formalism revealed that the enhancement is due to the stabilization of higher-lying 2P-active states, which are dominated by the excitations involving orbitals extending onto the carbonyl groups. Furthermore, calculations predicted even stronger stabilization of the 2P-allowed *gerade*-states in symmetric Pt octaalkoxycarbonyl-tetrabenzoporphyrins. Experiments confirmed that the 2PA cross-section of PtTBP$(CO_2Bu)_8$ near 810 nm reaches above 500 GM in spite of its completely centrosymmetric structure. Combined with exceptionally bright phosphorescence (ϕ_{phos} = 0.45), strong 2PA makes Pt(II) complexes of π-extended porphyrins a valuable class of chromophores for 2P applications. Another important advantage of these porphyrinoids is their compact size and easily scalable synthesis.

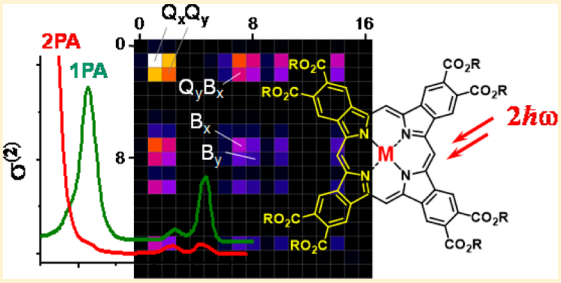

INTRODUCTION

Several applications of porphyrins rely on their ability to form triplet excited states. These include organic light-emitting diodes (OLED),[1,2] optical power limiting,[3−5] sensitized triplet−triplet annihilation,[6,7] photodynamic therapy (PDT)[8,9] and sensing of molecular oxygen.[10−13] In some cases, such as organic light-emitting diodes and imaging probes, strong phosphorescence from these states is required; in others triplet states do not need to be emissive, but instead must carry out photochemical transformations. In general, high yield of triplet formation and absence of intramolecular triplet quenching pathways are common requirements for these applications.

Both phosphorescent imaging probes and PDT agents must be able to absorb light in the near-infrared (NIR) spectral region in order to allow sub-surface excitation in biological tissues. One method to achieve such excitation is based on coherent two-photon absorption (2PA),[14] a nonlinear optical process, whose key feature is the quadratic dependence of the absorption rate constant (α) on the excitation flux (Φ), $\alpha = \sigma^{(2)}\Phi^2$, where the proportionality coefficient $\sigma^{(2)}$ is known as two-photon absorption cross-section (measured in Göppert−Mayer units: 1 GM = 10^{-50} cm^4 s molecule^{-1} photon^{-1}). In

Received: August 31, 2016
Published: November 7, 2016

DOI: 10.1021/jacs.6b09157
J. Am. Chem. Soc. 2016, 138, 15648−15662

biological tissues coherent 2P excitation is generally inefficient at depths beyond ~1 mm due to the strong scattering;[15] however, there are many biologically relevant experiments, especially in the area of neuroscience, where focusing light under the tissue surface even at depths not exceeding 500 μm is extremely desirable.[16−18] In addition, the ability to reduce out-of-focus excitation and minimize photodamage makes this method extremely attractive for both high-resolution imaging[19,20] and targeted tissue therapy.[21−23]

Over the past two decades 2PA properties of tetrapyrroles and related chromophores have been actively studied,[24−26] and a number of porphyrin-based systems with exceptionally high 2PA cross sections have been disclosed (see refs 24−26 for reviews and refs 27−37 for recent examples). Most of these new materials, however, have been designed with the PDT application in mind,[36,38−43] where the photochemical action is typically mediated by dark triplet states. In contrast, practically no information exists on 2P-absorbing porphyrins capable of emission of phosphorescence. Such molecules would be very useful as probes for two-photon phosphorescence lifetime microscopy (2PLM) of oxygen,[44] an emerging imaging technique with applications already encompassing several branches of biology.[45−51]

The 2PA cross sections of regular Pt and Pd porphyrins, which are routinely used as phosphorescent oxygen probes,[11−13] are typically quite low (~10 GM),[52,53] which makes these chromophores rather inefficient in 2P applications. To overcome this limitation over the past several years we have developed an approach to 2P antenna-enhanced phosphorescent probes, in which Pt porphyrins are excited indirectly by energy transfer from the appended 2PA chromophores.[44,53−55] Several nano-formulations constructed along the same principles have been reported later,[56−59] and conceptually similar core-antenna systems have been proposed as sensitizers for 2P PDT.[60,61] Unfortunately, polychromophoric systems suffer from a set of limitations, including undesirable triplet quenching pathways (e.g., intramolecular electron transfer[62]) and high cost of synthesis. Without doubt a much more practical solution would entail triplet probes possessing simultaneously bright phosphorescence and high 2PA. Potentially metal-to-ligand charge transfer (MLCT)-capable complexes of certain transition metals (e.g., Ru, Ir) may satisfy such criteria;[63−65] however, short lifetimes of MLCT states (<2 μs) render them relatively insensitive to oxygen in the physiological range of oxygen concentrations.

In centro-symmetric molecules, such as most metalloporphyrins, selection rules for one-photon (1P) and 2P transitions are mutually exclusive. Therefore, strongly 1P-allowed B (Soret) and Q states in porphyrins[66] are inaccessible by 2PA. These parity selection rules, however, should be relaxed upon lowering the symmetry of the porphyrin electronic system—an effect explored in some previous studies.[38,67−69] Recently we described the synthesis of Pt(II) porphyrins, in which the center-of-inversion symmetry is broken by way of asymmetric *syn*-fusion of the macrocycle with benzo and naphtho groups.[70] Here we report a study of these asymmetric molecules, comparing them with regular porphyrins as well as with symmetric π-extended porphyrins. Our 2PA cross-section measurements for the first time made use of time-resolved detection of phosphorescence, which permitted direct monitoring of the triplet states formed upon two-photon excitation, having the advantage of extremely low background noise. To interpret our findings we used the sum-over-states (SOS) method for calculation of 2PA spectra, combined with the TDDFT approach and *a posteriori* Tamm−Dancoff approximation (ATDA)[71−73] to compute the state-to-state and static electric dipole operator matrix elements for the SOS expression. This method was recently demonstrated to produce accurate values for both 2PA cross sections[73] and permanent dipole moments for excited states.[72] The computed 2PA spectra were found to be in close agreement with experimental data for a large number of chromophores.[74−83] In the present study, calculations based on this methodology not only helped us rationalize the observed experimental trends, but enabled an accurate prediction of 2PA in several porphyrin molecules prior to their synthesis and experimental evaluation. This combination of experiment and theory led to the identification of readily accessible potent 2PA chromophores with exceptionally bright phosphorescence.

EXPERIMENTAL METHODS

General. Porphyrins **1**−**6** were synthesized and purified as described previously.[70,84,85] The synthesis and characterization of porphyrin **7** can be found in the Supporting Information (SI, p S7). Fluorescein, rhodamine 6G (R6G), and rhodamine B were obtained commercially (Eastman Kodak) and used as received. Solutions for optical measurements were prepared using spectroscopic grade methanol (MeOH), ethanol (EtOH), and dimethylacetamide (DMA). Quartz fluorometric cells (Starna Cells, 1 cm optical path length) were used in all optical experiments. Quantum yields were measured against fluorescence of R6G in EtOH (Φ_{fl} = 0.95).[86] All solutions of phosphorescent porphyrins were rigorously deoxygenated using ultrapure argon (Airgas, grade 5) and/or by several freeze−degas−thaw cycles. Measurements of the triplet lifetimes revealed that these two methods were equally effective in removing traces of oxygen.

Molar Extinction Coefficients. Concentration of Pt(II) in solutions used for molar extinction measurements was determined by inductively coupled plasma atomic emission spectroscopy (ICP-OES). Based on the synthetic and purification protocols used,[70,87] Pt porphyrins were the only source of Pt(II) in these solutions. The ICP-OES method allows determination of the metal ion concentrations with precision of 0.01 ppm, where 1 ppm = $[m_{metal}(g)/m_{solution}(g)] \times 10^6$. In the case of Pt(II) in DMA, 1 ppm ≈ 4.77×10^{-8} M of Pt(II). The measurements were performed using Spectro Genesis ICP-OES instrument (Spectro Analytical Instruments GMBH; Kleve, Germany). Solutions of Pt(II) 2,4-pentanedionate (Alfa Aesar, 99.98% purity, 49.360% Pt content) in DMA (Pt concentrations: 0.54, 0.59, 1.18, 2.11, 5.10, 9.49, and 53.52 ppm) were used for the calibrations. The measurements were performed using a characteristic emission peak of Pt(II) ion at 306.474 nm. The calibrations were verified by independent measurements of the reference solutions of Pt(II) 2,4-pentanedionate in DMA with the concentrations of Pt varying in 0.5−5.0 ppm range. Absorbances of all porphyrin solutions were measured using the Perkin-Elmer Lamda 35 spectrophotometer.

Two-Photon Absorption (2PA) Cross Sections. For detailed description of the measurement setup see SI, p S3. The 2PA spectra of the phosphorescent Pt porphyrins were determined by the 2P excitation method. The measurements consisted of two steps. First, the 2P-induced phosphorescence of a selected "standard" porphyrin (porphyrin **5**) was measured and compared against the fluorescence of a chromophore with known 2PA cross-section (rhodamine B),[88,89] induced by the same excitation source in the same optical configuration. These measurements were performed at several excitation wavelengths, and the corresponding 2PA cross sections of the "standard" were calculated. In these experiments the excitation was by the continuous train of femtosecond (fs) pulses from a high repetition rate Ti:sapphire oscillator, while the emission was registered by a CCD-based spectrometer (Setup 1, Figure S1a).

Second, the phosphorescence of all Pt porphyrins, including the "standard", was measured in time-resolved fashion upon excitation by short (1−2 μs long) trains of fs pulses (excitation gates) using a single

DOI: 10.1021/jacs.6b09157
J. Am. Chem. Soc. 2016, 138, 15648−15662

PMT as a detector (Setup 2, Figure S1b). The calculation of the 2PA spectra consisted of the emission decays integration, normalization by the concentration, emission quantum yield and several other parameters (see SI for complete description) and comparing the result against the "standard". In principle, measurements of phosphorescence relative to fluorescence (as in Setup 1) could be performed for all Pt porphyrins; however, the proximity of the phosphorescence spectrum to the laser band, especially at shorter excitation wavelengths, resulted in large measurement errors due to the scattered laser background. In contrast, time-resolved registration permitted complete suppression of the scattered excitation and led to clean and reproducible 2PA spectra.

Quantum Chemistry Calculations. The quantum chemistry calculations were performed using in-house-modified Gaussian 09[90] in conjunction with M05-QX exchange-correlation functional. The latter was derived[91] by interpolation between M05 and M05-2X functionals.[92] M05-QX includes 35% of the exact exchange and is known to predict energies of electronic states with substantial charge transfer character more accurately than commonly used functionals, such as B3LYP. The SDD Stuttgart effective core potentials were used for the metal atoms,[93] while D95 basis set[94] with no diffuse functions was used for all other elements in order to prevent artificial Rydberg contributions to the valence excited states.[73,95] In all calculations the solvent effects were included using the dielectric continuum model in solvent model density (SMD) parametrization,[96] as implemented in Gaussian 09.

The energies and oscillator strengths were calculated using the time-dependent density functional theory (TDDFT). In order to compute resonant 2PA cross sections we combined the 2PA SOS formalism[97] with ATDA[71] applied to the second-order coupled electronic oscillators formalism.[98,99] The ATDA method uses CIS formulas for calculation of permanent dipole moments of excited states and transition dipole moments between the exited states. The ATDA method was implemented in the custom-modified version of the Gaussian 09 code. Unlike the CIS method that does not account for electron correlation and, therefore, often overestimates both permanent and transition dipole moments, TDDFT does account for electron correlation (albeit, implicitly). Consequently, TDDFT-computed values for permanent[72] and transition dipole moments[100,77] are significantly closer to those calculated by higher level methods, which include double-excitations explicitly (such as SAC-CI and EOM-CCSD). Also, being the second-order TDDFT, the ATDA method includes the manifold of true double excited states, which are missing from, e.g., CIS calculations.[100]

In this work, transitions to 22 excited states were calculated for all molecules. The dumping constant Γ (the same value for all states; eqs 1, 2, and S5) was 0.1 eV. For visual comparison with the experimental spectra, the computed discrete spectra were broadened by convolution with a Lorentzian function using Γ = 0.1 eV as well. For additional details see SI, pp S6 and S19.

RESULTS AND DISCUSSION

Theoretical Background. 2PA in porphyrins and related chromophores has been addressed extensively in the literature,[101−106] including effects of symmetric and asymmetric substitution,[67,68,107−109] resonant enhancement,[102,110−113] stabilization of 2P-allowed *gerade* states[102] and, most recently, analysis of vibronic contributions to 2PA.[105] The theoretical background of 2PA has been covered in several of these articles as well as in some general reviews.[114,115] Here for consistency we summarize only the key elements of the theory as it applies specifically to porphyrins, while the reader is referred to the dedicated theoretical work for details.

The SOS expression[14] relates the molecular 2PA cross-section ($\sigma^{(2)}$) to the quantity known as two-photon tensor $\mathbf{S}^{(f)}$ (eq 1; see SI, p S18):[116,117]

$$\sigma_{f0}^{(2)} \approx \omega_1\omega_2 |\mathbf{S}^{(f)}|^2 \rho_f(\omega_1 + \omega_2 - \omega_f),$$
$$|\mathbf{S}^{(f)}|^2 = \left| \sum_i \left[\frac{(\mathbf{e}_1\cdot\boldsymbol{\mu}_{i0})(\boldsymbol{\mu}_{fi}\cdot\mathbf{e}_2)}{E_i - \hbar\omega_1 + i\Gamma_i} + \frac{(\mathbf{e}_1\cdot\boldsymbol{\mu}_{i0})(\boldsymbol{\mu}_{fi}\cdot\mathbf{e}_2)}{E_i - \hbar\omega_2 + i\Gamma_i} \right] \right|^2 \quad (1)$$

In eq 1, $\sigma_{f0}^{(2)}$ is the 2PA cross-section for the transition from the ground state (ψ_0) to the final state (ψ_f); $\rho_f(\omega_1 + \omega_2 - \omega_f)$ is the line shape function for that transition ($\psi_0 \rightarrow \psi_f$); $\boldsymbol{\mu}_{mn} = \langle\psi_m|\boldsymbol{\mu}|\psi_n\rangle$, i.e., vectors with components (μ^x_{mn}, μ^y_{mn}, μ^z_{mn}), are the matrix elements of the electric dipole operator $\boldsymbol{\mu}$; and $\mathbf{e}_1$ and $\mathbf{e}_2$ are the unit polarization vectors of the two photons with energies $\hbar\omega_1$ and $\hbar\omega_2$, respectively. Index "i" in eq 1 runs over *intermediate* states ψ_i with energies E_i, which are all the eigenstates of the molecular Hamiltonian, including ψ_0 and ψ_f. The damping constant Γ_i is associated with the line shape of the intermediate state ψ_i, and is commonly set in calculations to an arbitrary chosen small value.[101] eq 1 can be obtained by solving the time-dependent Schrödinger equation using perturbative expansion to the second order and external potential in the form of oscillating electrical field.[14,118]

Orientational averaging applied to eq 1 leads to an expression applicable to randomly oriented molecules and photons of different polarizations.[119,120] For the case of *degenerate* 2PA, i.e., when the photon energies ($\hbar\omega_1$ and $\hbar\omega_2$) and polartizations ($\mathbf{e}_1$ and $\mathbf{e}_2$) are identical, eq 1 has a more compact form:

$$|\mathbf{S}^{(f)}|^2 = 4 \left| \sum_i \left[\frac{(\mathbf{e}\cdot\boldsymbol{\mu}_{i0})(\boldsymbol{\mu}_{fi}\cdot\mathbf{e})}{E_i - \hbar\omega + i\Gamma_i} \right] \right|^2 \quad (2)$$

The corresponding expansion for randomly oriented molecules and photons polarized linearly and parallel to each other is given by the double-summation:[117]

$$|\mathbf{S}^{(f)}|^2 = \frac{4}{15} \sum_i^N \sum_j^N S_{ij}^{(f)} \quad (3)$$

where $S_{ij}^{(f)}$ are products of the transition dipole moments connecting states ψ_0, ψ_f, ψ_i, and ψ_j (SI, p S18). This expression has been used in the past to calculate two-photon absorptivities of different kinds of chromophores, including tetrapyrroles.[67,68,101,104,105,117,121] In the present work the SOS expression was combined with the ATDA[71] to the second-order TDDFT. This method enabled computation of the matrix elements $\boldsymbol{\mu}_{nm}$, some of which are not available in the first-order TDDFT.[122] In the past this methodology has been shown to predict 2PA spectra in close agreement with experiment.[75,78,81,123]

The parity selection rule for 2P transitions follows directly from eqs 1 and 2. It is well-known that in systems with center-of-inversion symmetry, one-photon (1P) electric dipole transitions are allowed between states of opposite parity, i.e., *gerade* → *ungerade* ($g \rightarrow u$) or *ungerade* → *gerade* ($u \rightarrow g$). Since the ground state wave functions ψ_0 in closed-shell centro-symmetric molecules are of *g*-symmetry, the matrix elements $\boldsymbol{\mu}_{i0}$ will have nonvanishing values only if ψ_i are *u*-states, and, applying the same rule once again, the final states ψ_f must be *g*-states for nonzero values of $\boldsymbol{\mu}_{fi}$. Thus, 2P-transitions are allowed between states of equal parity ($g \rightarrow g$ or $u \rightarrow u$), i.e., the selection rules for 1P and 2P transitions in centro-symmetric systems are mutually exclusive.

While accurate calculations of 2PA properties require inclusion of as many states ψ_i as possible into eq 1, truncated

DOI: 10.1021/jacs.6b09157
J. Am. Chem. Soc. 2016, 138, 15648−15662

expressions of the two-photon tensor along with symmetry considerations are very instrumental in developing qualitative understanding of 2PA.[115,77] Porphyrins typically exhibit four low-lying absorption bands, Q_x, Q_y (in the region of 500−550 nm) and B_x, B_y (near 400 nm), where indexes x and y refer to the transitions' polarization in the macrocycle plane (x−y) (Figure 1a,b).[66]

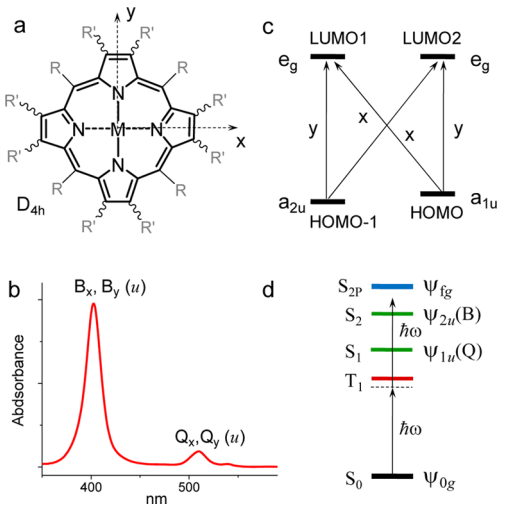

Figure 1. (a) Structure of a symmetric (D_{4h}) metalloporphyrin; axes show directions of the transitions' polarizations in the macrocycle plane.[66] (b) Typical linear (1P) optical absorption spectrum of a metalloporphyrin. (c) Excitations between pairs of quasi-degenerate HOMOs and LUMOs that give rise to excited states: Q state and B state. (d) Schematic state energy diagram showing partially 1P-allowed singlet Q state (*ungerade*; green), strongly 1P-allowed singlet B state (*ungerade*; green), a 2P-allowed singlet state (*gerade*; blue) and the lowest triplet state T_1 (dark red). Arrows with symbols "$\hbar\omega$" depict the two photons in the 2P excitation process.

Q_x, Q_y and B_x, B_y transitions are pairwise degenerate in ideally symmetric porphyrins (D_{4h}, e.g., in metalloporphyrins) or nearly degenerate in less symmetric systems (e.g., free-base porphyrins, D_{2h}). Consequently, the Q_x, Q_y and B_x, B_y pairs are usually referred to collectively as Q and B bands. According to the Gouterman's four-orbital model,[66,124] which has been corroborated over the years by numerous *ab initio* calculations, the corresponding singlet excited states (labeled by the same symbols as the transitions) are formed as a result of configuration interaction of single-electron excitations between two quasi-degenerate HOMOs (b_{1u} and b_{2u}) and two quasi-degenerate LUMOs (e_g) (Figure 1c). In the plain unsubstituted porphyrin (porphine) the transition to the upper B state is strongly allowed ($\varepsilon > 2 \times 10^5$ M^{-1} cm^{-1}), while the Q transition is forbidden. However, substitution into either the *meso*-positions or pyrrolic rings partially lifts the orbital degeneracy, and the Q band becomes enhanced via the so-called intensity borrowing effect.[124] In practice, the extinction coefficients of porphyrins in the Q band region are in the range of 10^4 M^{-1} cm^{-1}, but can reach $>10^5$ M^{-1} cm^{-1}, depending on the substitution.

Both B and Q states are mixtures of u-orbital configurations. Therefore, these states are not allowed for 2PA. The strongly 2P-allowed g-states in porphyrins typically lie at higher energies than the B state (Figure 1d).[66,101,105] Unfortunately, experimental observation of 2P-excitation into these states is not possible because of the much stronger linear absorption into the Q state, which becomes dominant when the laser energy ($\hbar\omega$) approaches half the energy of the 2P allowed transition(s).

A common framework for qualitative analysis of 2PA in centro-symmetric molecules considers only three states in the expression for $\mathbf{S}^f_0$ (eq 2) (the three-state model):[115,125] the ground state (ψ_{0g}), the lowest 1P-allowed state (ψ_{1u}) and the final 2P state (ψ_{fg}):

$$|\mathbf{S}^{(f)}|^2 \approx \left| \frac{(\mathbf{e}\cdot\boldsymbol{\mu}_{00})(\boldsymbol{\mu}_{f0}\cdot\mathbf{e})}{E_0 - \hbar\omega + i\Gamma_0} + \frac{(\mathbf{e}\cdot\boldsymbol{\mu}_{f0})(\boldsymbol{\mu}_{ff}\cdot\mathbf{e})}{E_f - \hbar\omega + i\Gamma_f} + \frac{(\mathbf{e}\cdot\boldsymbol{\mu}_{10})(\boldsymbol{\mu}_{f1}\cdot\mathbf{e})}{E_1 - \hbar\omega + i\Gamma_1} \right|^2 \quad (4)$$

Neglecting the higher-lying states is justified by the fact that the corresponding terms in eq 2 become progressively smaller as the detuning factor (E_i−$\hbar\omega$) increases. In eq 4, $\boldsymbol{\mu}_{00} = \langle\psi_0|\boldsymbol{\mu}|\psi_0\rangle$ and $\boldsymbol{\mu}_{ff} = \langle\psi_f|\boldsymbol{\mu}|\psi_f\rangle$ are the expectation values of the electric dipole operator on states ψ_0 and ψ_f, which are the static dipole moments $\mathbf{p}_0$ and $\mathbf{p}_f$, respectively. Since the molecule is symmetric, $\mathbf{p}_0$ and $\mathbf{p}_f$ are effectively zero, and the first two terms in eq 4 cancel out.

In relation to porphyrins the truncated SOS expression in principle should include two intermediate states, B and Q (Figure 1d):

$$|\mathbf{S}^{(f)}|^2 \approx \left| \frac{(\mathbf{e}\cdot\boldsymbol{\mu}_{Q0})(\boldsymbol{\mu}_{fQ}\cdot\mathbf{e})}{E_Q - \hbar\omega + i\Gamma_Q} + \frac{(\mathbf{e}\cdot\boldsymbol{\mu}_{B0})(\boldsymbol{\mu}_{fB}\cdot\mathbf{e})}{E_B - \hbar\omega + i\Gamma_B} \right|^2 \quad (5)$$

although usually only the lowest excited state, the Q state, is considered explicitly. For example, Drobizhev, Rebane and co-authors[102,110−113] have shown that in certain cases 2PA above the B band region is dominated by the resonance enhancement effect, i.e., the proximity of the laser energy to the Q state and, therefore, small value of the denominator in the first term of eq 5 (Figure 1d). Factors increasing the transition dipole moments $\boldsymbol{\mu}_{Q0}$ and $\boldsymbol{\mu}_{fQ}$ naturally also help to increase $\sigma^{(2)}$.[111,126] Furthermore, in porphyrins possessing strong donor−acceptor character the difference between the static dipole moments in the ground and excited states ($\mathbf{p}_0$ and $\mathbf{p}_f$) may become non-negligible, so that the corresponding terms (eq 4) may also become significant contributors to 2PA.[34,107,127]

Although rarely considered in the analysis, the B state plays an important role in 2PA of porphyrins.[105,111] First, the B state is responsible for the intensity enhancement of the Q band transition ($\boldsymbol{\mu}_{Q0}$) via the intensity borrowing effect.[124] Second, although the denominator (E_B−$\hbar\omega$) is larger than (E_Q−$\hbar\omega$) (Figure 1d), the dipole strength $\boldsymbol{\mu}_{B0}$ is usually significantly higher than $\boldsymbol{\mu}_{Q0}$ (Figure 1b), which can make up for a non-negligible contribution of the B state pathway to the overall value of $\sigma^{(2)}$.

Finally, it should be mentioned that in complexes of porphyrins with metals that induce strong spin−orbit coupling, such as in Pt porphyrins, direct $S_0 \rightarrow T_1$ linear absorption may gain significant dipole strength (e.g., $\varepsilon \approx 100$ M^{-1} cm^{-1}),[62,128] thereby limiting the effective range of experimental 2PA measurements. As the excitation energy in a 2PA experiment approaches the triplet state (Figure 1d), $S_0 \rightarrow T_1$ absorption becomes strong and usually overshadows 2PA to the higher-lying states.

Based on the above considerations, our original intention was to examine whether breaking the symmetry of the macrocycle can relax the parity selection rules and partially allow 2PA to

DOI: 10.1021/jacs.6b09157
J. Am. Chem. Soc. 2016, 138, 15648−15662

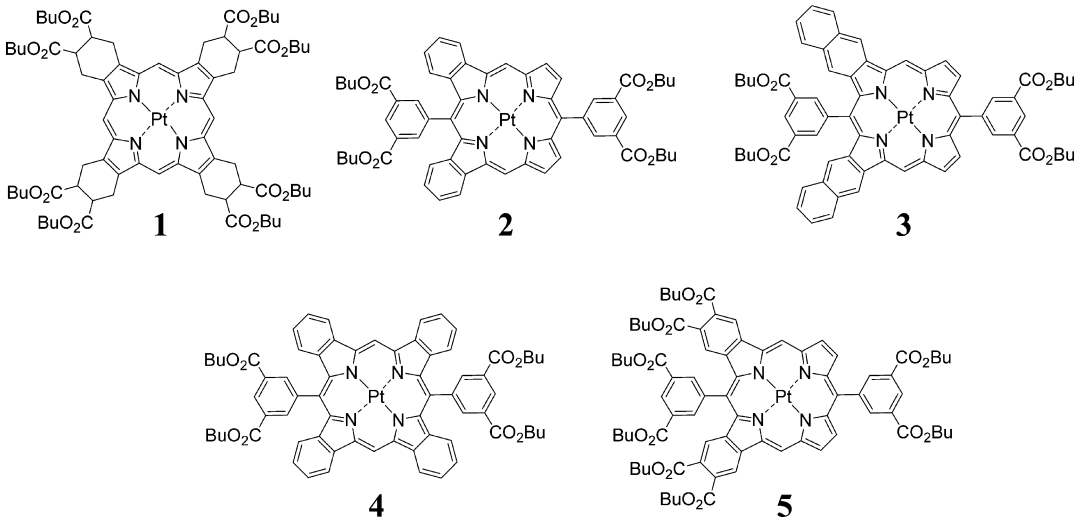

Figure 2. Structures of the studied Pt porphyrins.

1P-allowed Q and B states in phosphorescent metalloporphyrins. Aromatic π-extension offers a convenient method to lower the symmetry of the porphyrin macrocycle and is known to profoundly affect the porphyrin electronic structure. As the study progressed it became apparent that factors other than symmetry play perhaps even more important role in defining 2PA properties of our set of compounds. These effects were investigated both experimentally and computationally using several model systems.

Choice of Model Compounds. The structures of the first set of Pt(II) porphyrins studied in this work are shown in Figure 2. In all cases, the peripheral butoxycarbonyl groups were used to enhance the solubility of the porphyrins in organic solvents and prevent their aggregation. According to our previous studies,[70,84] butoxycarbonyl-substituted porphyrins do not aggregate in dimethylformamide (DMF), dimethylacetamide (DMA), tetrahydrofuran (THF), and several other aprotic solvents.

The compounds shown in Figure 2 enabled the following comparisons. First, by comparing fully symmetric nonextended porphyrin **1** (D_{4h})[55,84] with *syn*-dibenzo- and *syn*-dinaphthoporphyrins **2** and **3** (C_{2v})[70] we examined how the change in the symmetry affects the 2PA. The fully symmetric tetrabenzoporphyrin **4**[85] served as a reference to establish whether benzo-extension by itself has any significant influence on 2PA unrelated to the symmetry effects. One additional point for the comparison was Pt tetraaryltetrabenzoporphyrin ($PtAr_4TBP$, SI, p S19); although, as expected it was found to exhibit 2PA spectra very similar to those of its diaryl analogue **4**.

Second, four butoxycarbonyl groups (CO_2Bu) in the *syn*-benzo rings induce strong static dipole moment in porphyrin **5** as compared to **2**. As mentioned, static polarization may result in a significant enhancement of 2PA (eq 4), and the role of this effect could be examined using **5** and **2** as models.

Third, in addition to polarizing the molecule, carbonyl groups in **5** are in partial conjugation with the macrocycle, and that could exert its own influence on 2PA. As we show below, the interaction of the carbonyl groups with the macrocycle indeed turned out to make the most dominant contribution to the 2PA properties of the substituted benzoporphyrins.

Linear (1P) Photophysical Properties. The 1P absorption and phosphorescence emission spectra of the Pt porphyrins are shown in Figure 3, and the corresponding data are summarized in Table 1. Linear absorption data are

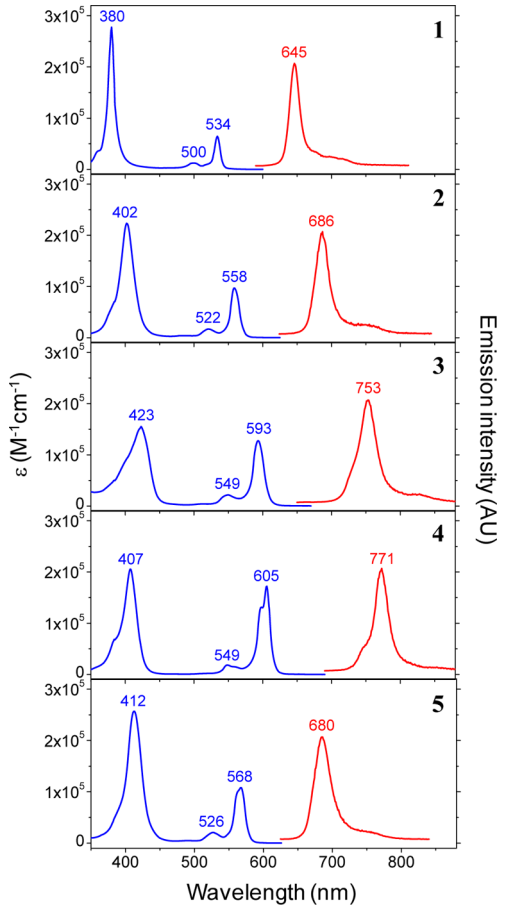

Figure 3. Steady state absorption (blue line) and phosphorescence (red line) spectra of Pt porphyrins in DMA.

important not only for practical measurements of 2PA, but also for quantitative interpretation of 2PA spectra: the excited state energies and the corresponding transition dipole moments directly factor into the value of $\sigma^{(2)}$ via eqs 1–4. To minimize errors in determination of molar extinction coefficients (ε) of

DOI: 10.1021/jacs.6b09157
J. Am. Chem. Soc. 2016, 138, 15648–15662

Table 1. Selected Photophysical Properties of the Studied Pt Porphyrins[a]

compd no.	λ_{max} Q λ_{max} B (nm)	E_{max} Q E_{max} B (eV)	ε_{max} Q ε_{max} B (M^{-1} cm^{-1})	f_{Q0}[b] f_{B0}	λ_{max} p[c] (nm)	E_{max} T_1 (eV)	$2J$[d] (eV)	ϕ_p[c,e]	τ[f] (μs)	k_r (s^{-1})	k_{nr} (s^{-1})	k_r/k_{nr}
1	534 380	2.32 3.26	60550 277350	0.17 1.36	645	1.92	0.40	0.43	101	4257	5643	0.75
2	558 402	2.22 3.08	84460 223210	0.27 1.69	686	1.81	0.41	0.40	91	4396	6593	0.67
3	593 423	2.09 2.93	127560 155290	0.44 1.92	753	1.65	0.44	0.23	50	4600	15400	0.30
4	605 407	2.05 3.05	168120 205450	0.49 1.73	771	1.61	0.44	0.23	65	3538	11847	0.30
5	568 412	2.18 3.01	98930 256830	0.37 2.04	680	1.82	0.36	0.45	78	5769	7051	0.82

[a]All measurements were performed in DMA and 22 °C. [b]f is oscillator strength. [c]"p" represents phosphorescence. [d]S_1-T_1 gap. [e]ϕ_p is the phosphorescence quantum yield. [f]τ is the triplet state lifetime.

porphyrins, we measured the concentrations of the samples used in both ε and later $\sigma^{(2)}$ measurements by ICP-OES, because ICP-OES allows measurements of metals in solutions with 0.01 ppm precision (see Experimental Methods). Considering the synthetic and purification protocols used, Pt porphyrins were the only source of Pt(II) ion in our samples.

The second relevant experimental detail is concerned with measurements of emission quantum yields. Due to the very strong spin−orbit coupling the triplet states (T_1) in Pt(II) porphyrins form with nearly unity efficiency.[129,130] As a result, the only observable emission from Pt(II) porphyrins in solutions at ambient temperatures is $T_1 \rightarrow S_0$ phosphorescence, which occurs on the microsecond time scale (typically tens of microseconds).[130] Unfortunately, the literature data on the phosphorescence quantum yields of porphyrins are highly unreliable. The reported values can vary by as much as 3−4 times for the same compound, even when measurements are reported to have been performed under nearly identical conditions. The discrepancies usually stem from the use of different actinometers (luminescent standards) as well as from miscalibrated detectors (photomultipliers or integrating spheres) employed for quantum yield measurements. For example, we have found that our own measurements of the quantum yields of some Pt porphyrins[70] were in fact inaccurate due to the errors in the detector sensitivity correction data provided by the instrument manufacturer. To avoid this and similar errors, in the present work we first measured the detector sensitivity curve using a standard NIST-calibrated light source and then referenced all the measured emission intensities to the same actinometer (porphyrin **5**), whose quantum yield (ϕ_p) was in turn determined against a well-documented fluorescent standard R6G. The phosphorescence quantum yield of **5** was confirmed to be virtually independent of the excitation wavelength throughout the Q band region. Highly reproducible values of the fluorescence quantum yield of R6G (in EtOH at 22 °C) were reported by several groups (ϕ_{fl} = 0.94−0.95).[86,131] All the quantum yield measurements were performed according to the published guidelines,[132] and the values were reproduced several times, converging with less than 10% error.

The linear photophysical properties of compounds in Figure 2 generally follow the well-known trends.[4,133−136] Fusion of the macrocycle with external aromatic rings leads to two interrelated phenomena: bathochromic shifts of the absorption bands and increase in the oscillator strength of the Q band relative to the B band. The common origin of these effects is the destabilization of one of the porphyrin HOMO (b_{1u}), which is localized predominantly on the β-pyrrolic carbons. Lifting the degeneracy lowers the excitation energy and simultaneously causes increase in the intensity borrowing to benefit the Q band.[124,134]

In going from **1** to **3** both these effects are clearly observable. Compared to nonextended porphyrin **1**, **2** and **3** exhibit bathochromically shifted maxima and increased Q band intensities. Noticeably, the Q band remains narrow and symmetric throughout the series, indicating that the Q_x and Q_y transitions are degenerate, which is consistent with equal elongation of the macrocycle in both *x*- and *y*-directions. In contrast, in *anti*-dibenzoporphyrins the *x*- and *y*-transition dipole moment vectors are unequal, resulting in multiple spectral lines in Q and B band regions.[137] The spectrum of *syn*-dinaphthoporphyrin **3** approaches that of symmetric tetrabenzoporphyrin **4**, which according to the simple "particle-in-a-box" analogy reflects the fact that the transition dipole lengths in these two porphyrins are nearly equal. The B band of **3** is significantly broadened, resembling the spectra of metallo-[2,3]-tetranaphthoporphyrins.[84,136] It is known that the four-orbital approximation breaks down for naphthoporphyrins, and their B states include significant contributions of higher energy orbitals.[4,133]

The emission quantum yields decrease, as expected, from **1** to **3** as the energy T_1-S_0 gap decreases. The $T_1 \rightarrow S_0$ intersystem crossing is additionally enhanced by nonplanar deformations of the macrocycle, which are induced by the *meso*-aryl substituents. The nonplanarity facilitates coupling between the *meso*-aryl groups and the macrocycle electronic system,[138] further lowering the excited state energy and at the same time making the porphyrin skeleton more flexible. The low-energy out-of-plane vibrations are known to greatly promote non-radiative relaxation of both singlet[139,140] and triplet[135] states. Although *meso*-5,15-diaryl-substituted porphyrins are much less

DOI: 10.1021/jacs.6b09157
J. Am. Chem. Soc. 2016, 138, 15648−15662

Table 2. Experimental Two-Photon Absorption Properties of Pt Porphyrins and Calculated Energies, Oscillator Strengths, and 2PA Cross Sections of the Their Low-Lying Singlet Excited States[a,b]

	experimental					calculated				
compd no.	λ_{max}^{2P} [c] (nm)	$\sigma_{max}^{(2)}$ [d] (GM)	$\sigma_B^{(2)}$ [e] (GM)	$E_Q - \hbar\omega$ [f] (eV)	$E_{T1} - \hbar\omega$ [g] (eV)	state	E singlets [h] (eV)	λ [i] (nm)	f [j]	$\sigma^{(2)}$ [k] (GM)
1	1000	1.3	1.0	1.08	0.68	S_1, S_2 (Q)	2.59, 2.59	478, 478	0.03, 0.03	0.0, 0.0
						S_7, S_8 (B)	3.46, 3.46	358, 358	1.52, 1.52	0.0, 0.0
2	750	56.8	10.9	0.57	0.15	S_1, S_2 (Q)	2.46, 2.49	503, 499	0.12, 0.11	0.8, 1.0
						S_6, S_7 (B)	3.28, 3.33	378, 372	1.86, 0.92	7.7, 0.0
						S_9	3.61	343	0.00	28.3
						S_{12}	3.65	339	0.01	44.4
						S_{18}	4.25	291	0.03	50
						S_{19}	4.32	287	0.00	501
3	860	46.2		0.65	0.20	S_1, S_2 (Q)	2.32, 2.36	535, 524	0.29, 0.28	7.7, 0.1
						S_4, S_5 (B)	3.14, 3.15	395, 393	1.42, 0.73	25.5, 5.6
						S_6, S_7	3.20, 3.23	388, 384	0.13, 0.19	12.5, 69.0
						S_8	3.30	375	0.32	10.2
						S_9	3.40	364	0.00	67.8
						S_{10}, S_{11}	3.55, 3.55	350, 349	0.22, 0.01	56.3, 173
						S_{12}	3.60	345	0.10	198
4	860	17.4		0.61	0.17	S_1, S_2 (Q)	2.27, 2.29	546, 541	0.38, 0.34	0.0, 0.0
						S_6, S_7 (B)	3.28, 3.30	378, 376	1.26, 1.72	0.0, 0.0
						S_8	3.32	373	0	20.1
						S_9	3.40	365	0	2.8
5	750	213	12.7	0.53	0.17	S_1, S_2 (Q)	2.42, 2.44	512, 508	0.15, 0.10	0, 5.0
						S_5, S_6 (B)	3.12, 3.17	398, 391	0.69, 1.76	4.0, 2.0
						S_{10}	3.55	349	0.02	27.0
						S_{11}	3.69	336	0.00	12.0
						S_{12}	3.83	324	0.01	328

[a]For complete data sets see SI, p S20. [b]All measurements were performed in DMA and 22 °C. [c]Excitation wavelength at which the maximal 2PA cross-section was observed and [d]its value. [e]Experimental 2PA cross-section at the B band maximum. [f]Detuning factor ($E_Q - \hbar\omega$) for the Q state pathway at the excitation wavelength λ_{max}^{2P}. [g]Difference between the excitation energy and the energy of the lowest triplet state (T_1). [h]Energies of singlet states S_n. Closely spaced states are grouped on the same line; only states relevant to the discussion are shown. [i]Wavelengths corresponding to 1P excitation. For 2P excitation these values should be doubled. [j]Oscillator strengths (for $S_0 \rightarrow S_n$). [k]2PA cross sections.

distorted than their tetraaryl-substituted analogues,[135] some nonplanarity is still present in **2** and **3**[70] compared to essentially planar compound **1**.

Butoxycarbonyl groups in porphyrin **5** induce non-negligible bathochromic shifts of both B and Q bands relative to those of unsubstituted **2**, while the phosphorescence maximum shifts hypsochromically. These tendencies are consistent with the expansion of the conjugation onto the carbonyl groups, which destabilize one of the HOMOs as well as reduce the exchange energy ($2J$) by ~0.05 eV as a result of the enlargement of the whole π-system.[141] The carbonyls also act to further enhance the spin−orbit coupling in **5**, promoting both the nonradiative (k_{nr}) and radiative (k_r) triplet decays, but fortunately favoring the latter. As a result, the triplet emissivity of *meso*-diaryl-substituted porphyrins **2** and **5** is among the highest reported to date, consistent with previous measurements.[70,135]

Two-Photon (2P) Absorption. The 2PA properties of the porphyrins are summarized in Table 2 (for complete list of the computed states, energies, oscillator strengths, and 2PA cross sections see SI, p S20). To facilitate comparison, the 2PA spectra are shown in Figure 4 superimposed on the corresponding linear spectra. The 2PA measurements were performed by the relative emission method. The porphyrin samples (typically 3−4 μM) were excited by 1-μs-long trains of femtosecond pulses (~80 pulses per train), and the phosphorescence was recorded in time-resolved fashion (see SI, p S3, for details). This approach is similar to the conventional two-photon fluorescence method,[89] except that time-resolved detection, made possible by the long triplet lifetimes, allowed for much better rejection of the scattered laser background and greatly increased the SNR in the spectra. Removing the laser background by spectral filtering, as is commonly done in 2P excitation measurements,[89] is more prone to errors especially in the case of phosphorescence. The latter occurs very close of the laser spectrum when porphyrins are excited at the half the energy of the B state—a region of particular interest for 2PA. Nonetheless, in order to calibrate the phosphorescent standard (porphyrin **5**), its phosphorescence still had to be compared to the fluorescence of a chromophore with known 2PA cross-section (e.g., rhodamine B). For that the emission was acquired in the steady state regime and filtered spectrally to remove the laser background (see Experimental Methods for details). The excitation wavelength for the calibration was chosen to be in the far red (>900 nm) to minimize the laser interference.

DOI: 10.1021/jacs.6b09157
J. Am. Chem. Soc. 2016, 138, 15648−15662

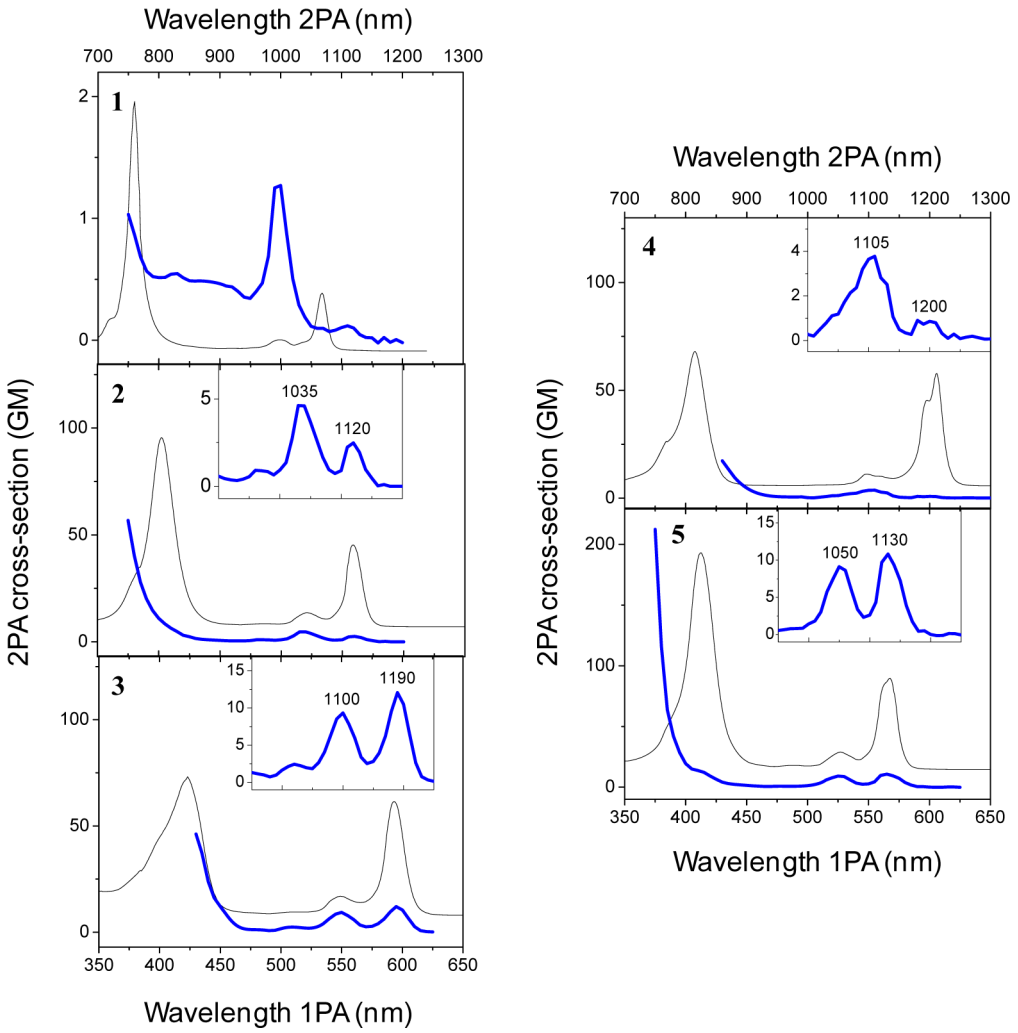

Figure 4. Two-photon absorption spectra of Pt porphyrins in DMA (blue lines) and the corresponding arbitrarily scaled linear absorption spectra (black lines).

All the 2PA spectra in Figure 4 exhibit similar features: low 2PA in the Q region and a pronounced rise near the B state. The blue edges of the spectra in all but one case (porphyrin **1**) correspond to the maximal attainable value of $\sigma^{(2)}$, designated as $\sigma^{(2)}_{max}$ (λ^{2P}_{max} is the corresponding wavelength). These spectral boundaries are defined by the interfering linear absorption directly into the triplet state ($S_0 \rightarrow T_1$). At wavelengths below λ^{2P}_{max}, the slope of the log−log plot of the signal power dependence decreased below 1.9, while everywhere throughout the spectral range shown in Figure 4 it was 2.0 ± 0.05. For porphyrin **1**, $\sigma^{(2)}_{max}$ was observed at one of the Q band vibronic maxima.

Common for all the compounds in the series the cross sections in the Q state region are relatively low, not exceeding 10−15 GM, while the relative intensities of the vibronic bands differ from those in the corresponding linear spectra. The latter tendency has been observed previously for different porphyrinoids,[102,105] and it is likely related to the symmetry of the corresponding vibrations, whereby an asymmetric mode promotes stronger 2PA.

As expected, asymmetric π-extension of the macrocycle causes an enhancement in the 2PA into 1P-allowed states. The centro-symmetric porphyrin **1** is a very weak 2P absorber, which agrees well with the previously published data on Pt porphyrins.[53] In going from **1** to **2** and **3**, the $\sigma^{(2)}$ values in both the Q and Soret band regions increase, but the effect is relatively moderate considering rather significant deviation of these porphyrins from the D_{4h} symmetry. From the continuous rise near the blue edge of the spectrum of **2** it is clear that stronger 2PA states are located above the B state level. Probably even stronger rise can be expected for dinaphthoporphyrin **3**, although in this case measurements above the B state were not possible due to the interfering linear absorption.

The absolute energies of the states predicted by the calculations (Table 2) were overestimated in all cases by ~0.2 eV. However, the trends in the spectra were reproduced rather well (for computed spectra see SI, p S20). In the case of porphyrin **2** moderate 2PA activity was predicted in the B state region (7.7 GM), while placing a stronger 2P absorbing state (S_9, 28.3 GM) by 0.3 eV higher in energy. For porphyrin **3** even stronger 2PA at the B state was predicted, correlating with larger deviation of this molecule from D_{4h} symmetry. In addition, stronger than in **2** rise could be expected toward 2PA-active states S_9−S_{12}, but unfortunately the low-lying triplet state prevented us from experimentally observing this absorption.

The experimental 2PA near the Q state of tetrabenzoporphyrin **4** was weak again, and the calculations predicted it to be nearly negligible, which is consistent with its high symmetry

DOI: 10.1021/jacs.6b09157
J. Am. Chem. Soc. 2016, 138, 15648−15662

and relatively high planarity.[135] In this case the measurement in the Soret region had to be truncated already at 860 nm due to the strong linear component, but a characteristic rise was still detectable above the B state level. This rise, according to the calculations, can be due to the moderately absorbing states S_8 and S_9, while a much larger 2P activity was predicted for state S_{11} (SI, p S24), which again is positioned significantly above the B state level. It is worth mentioning that the behavior of the symmetric $PtAr_4TBP$ (SI, p S19) is very similar to that of diaryltetrabenzoporphyrin **4**, although the former exhibits slightly higher 2PA value (~12 GM) near one of its Q band vibronic maximum. This mild enhancement may be related to the strong saddling distortion of $PtAr_4TBP$.[2,142] Nonplanarity effects on 2PA have been considered previously.[105] It is also worth a note that our results for $PtAr_4TBP$ differ from the previously reported values for analogous Zn tetraphenyltetrabenzoporphyrin ($ZnPh_4TBP$), whose $\sigma^{(2)}$ at the Q band maximum (650 nm) was found to be 90 GM,[102] i.e., more than 7 times higher than the value measured for $PtAr_4TBP$. The reason for such a large difference is unclear. By analogy with linear spectra one would expect that the effect of the metal ion on the macrocycle-centered transitions should be relatively minor. In the future it will be interesting to remeasure the cross sections of these two molecules using the same experimental system.

Overall, the main conclusion from this part of the study is that aromatic π-extension does increase 2PA in porphyrins, and the effect is more pronounced when the extension breaks the inversion symmetry. However, the 2PA into the B and Q states even in asymmetric porphyrins is still much weaker than the 2PA into higher-lying states. In Pt complexes these upper 2P-active states are inaccessible due to the interfering linear $S_0 \rightarrow T_1$ absorption.

The situation starts changing dramatically upon introduction of ester groups into the benzo-rings of the π-extended macrocycle. Comparing the spectra of direct analogues **2** and **5** we see immediately that in the case of **5** the rise in the blue region is much steeper, reaching at the edge 213 GM, compared to 57 GM for **2**. At the same time, the true 2PA maximum in **5** is still not reached, as it lies above the B state level. Considering that these two porphyrins have significantly different ground state static dipole moments (calc. 4.73 D for **5** vs 0.92 D for **2**), one could be tempted to correlate the higher 2PA of **5** with its stronger static polarization. However, according to eq 4 it is the squared difference between the ground and excited state dipole moments $\delta p^2 = |\mathbf{p}_f - \mathbf{p}_0|^2$ that contributes into $\sigma^{(2)}$ (eq 4). Calculations show that for **2** and **5** the values of δp^2 are similar and relatively small (<0.5 D^2) for both Q and B states as well as for higher-lying 2P-active states. Therefore, dipole moment is unlikely to explain the large increase in 2PA of **5**. Similarly, the resonance enhancement effect[110] can be ruled out, since the detuning factors for the Q state pathway ($E_Q - \hbar\omega$) in porphyrins **2** and **5** are essentially the same (Table 2).

It turns out that the main effect of butoxycarbonyl groups in **5** is stabilization of strongly 2P-active higher lying states, shifting them closer to the range accessible by 2P excitation. A qualitative illustration of this effect is shown in Figure 5. While the 2P maximum in **5** is still beyond the reach, the steeper and stronger rise at the blue edge of the spectrum indicates larger overlap between the 2P band and the laser line envelope. According to the calculations, in porphyrin **5** a state with moderate 2P activity (S_{10}, 3.55 eV, $\sigma^{(2)}_{calc} \approx 27$ GM) lies 0.06 eV

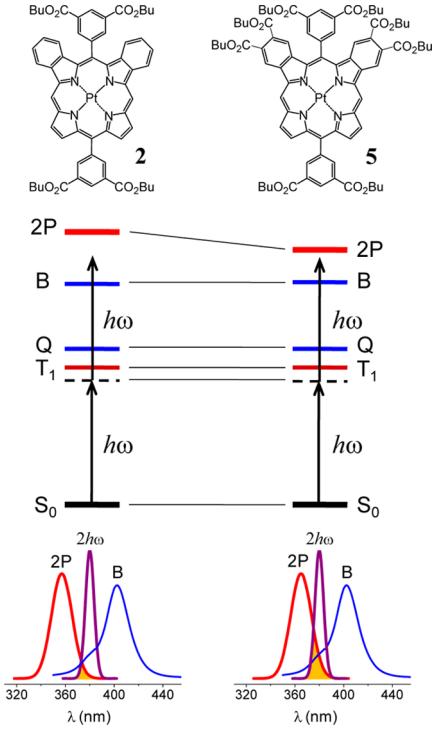

Figure 5. Energy state diagrams of Pt porphyrins **2** and **5** illustrating stabilization of 2P-active states in **5** due to the alkoxycarbonyl substituents.

lower than the corresponding state in **2** (S_9, 3.61 eV, 28.3 GM). More importantly, in **5** there is a strongly 2P-absorbing state S_{12} (3.83 eV, 328 GM), which lies 0.28 eV above the level of S_{10}. In contrast, in **2** the analogous 2P states (S_{18}, S_{19}) are lifted by more than 0.6 eV. Considering that the triplet states in **5** and **2** have essentially the same energies (1.82 vs 1.81 eV, Table 1), the separation between the 2P states and the highest attainable excitation frequency (which is set effectively by the level of the triplet) decreases, explaining the rise in the measured value of $\sigma^{(2)}$. Noteworthy, the oscillator strengths for these strongly 2P-active transitions in both **2** and **5** are nearly zero, indicating that approximate symmetry of the electronic structure still holds in spite of the fact that formally D_{4h} symmetry is broken.

The highly 2P-active states in porphyrins **2** and **5** (S_{19} and S_{12}, respectively) are superpositions of multiple orbital configurations. However, the leading configurations account for 72% and 87% of the transitions and correspond to the excitations HOMO → LUMO+6 and HOMO → LUMO+4 in **2** and **5**, respectively. The relevant Kohn−Sham MOs are shown in Figure 6, clearly illustrating the role of the alkoxycarbonyl substituents. The HOMOs in **2** and **5** are nearly identical. However, the LUMO+4 in **5** expands onto the carbonyls, whereas in **2** the corresponding MO (LUMO+6) is contained entirely within the benzo-extended macrocycle. It appears that this extra extended conjugation involving the carbonyl groups leads to the state stabilization and thereby causes a substantial increase in the 2PA.

Symmetric Octaalkoxycarbonyl-Substituted Tetrabenzoporphyrins. Having determined the reason for the enhancement of 2PA in alkoxycarbonyl-substituted dibenzoporphyrin **5**, we set out to examine whether the same effect is present in other alkoxycarbonyl-benzoporphyrins regardless of their symmetry. Calculations proved to be extremely useful in interpreting the 2PA properties, and at this point it was

DOI: 10.1021/jacs.6b09157
J. Am. Chem. Soc. 2016, 138, 15648−15662

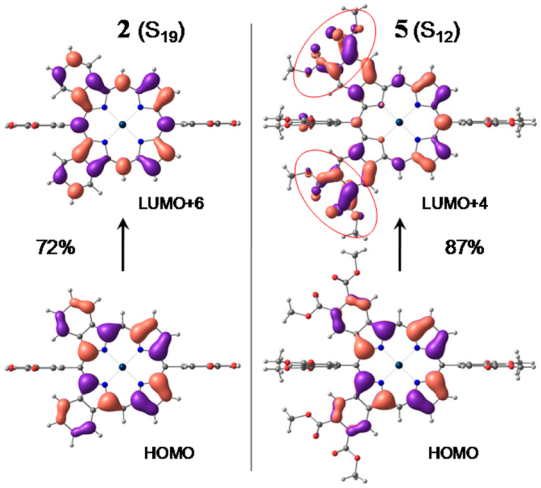

Figure 6. Kohn–Sham orbitals corresponding to the leading amplitudes in the 2P transitions in porphyrins **2** and **5**. The part of LUMO+4, which leads to the state stabilization in **5**, is circled in red.

interesting to perform a "blind test" by checking the ability of calculations to predict the spectra prior to conducting experimental measurements. The structures of two symmetric substituted Pt tetrabenzoporphyrins and their calculated 1P and 2P spectra are shown in Figures 7 and 9, below.

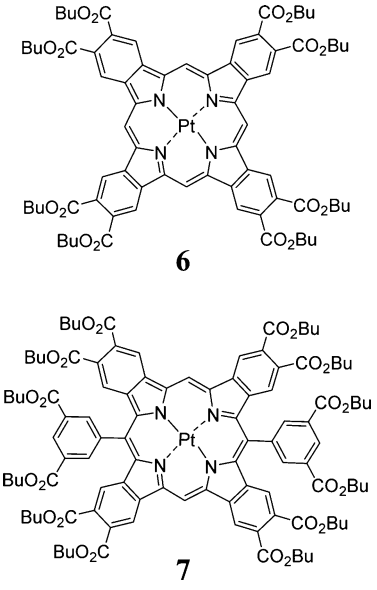

Figure 7. Structures of symmetric Pt octalkoxycarbonyl-substituted tetrabenzoporphyrins.

Tetrabenzoporphyrins without *meso*-aryl-substituents are known to exhibit especially high triplet emissivity.[87,135] Since one of our goals was to identify porphyrins possessing both large 2PA cross sections and high phosphorescence quantum yields, porphyrin **6** presented particular interest (Figure 7). It is worth noting that from the synthetic point of view octaalkoxycarbonyl-tetrabenzoporphyrins are probably the most accessible π-extended porphyrins known today. They can be readily synthesized by either the retro-Diels–Alder[143] or oxidative aromatization[144] methods. 5,15-Diaryltetrabenzoporphyrin **7** is the direct analogue of benzo-unsubstituted porphyrin **4**, and it was used for comparison. Both molecules are compact and can be easily functionalized for applications.

The calculations predicted existence of several 2P-active states in porphyrin **6** lying above the B state level. The first two states, S_6 and S_7 (Table 3), exhibit moderate 2PA cross sections; however, the transition to the next state S_8 was calculated to have the $\sigma^{(2)}$ value of 789 GM, which is more than two times higher than the maximal 2PA in non-centrosymmetric porphyrin **5**. The 2P-absorbing state in **6** has energy of 3.49 eV and involves predominantly one configuration (Figure 8): HOMO → LUMO+2 (89%), while other configurations

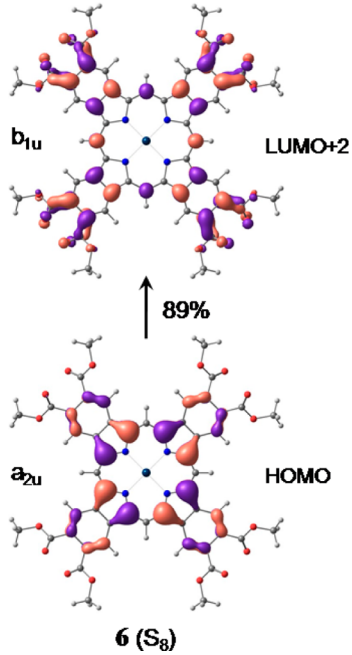

Figure 8. Kohn–Sham orbitals comprising the leading configuration in the lowest energy 2P-active state (S_8) in centrosymmetric Pt tetrabenzoporphyrin **6**.

together constitute less than 3% (per excitation) of the overall transition amplitude. Just like in porphyrin **5**, the target orbital in **6** (LUMO+2) extends outward to the carbonyl groups, while the HOMO is contained entirely within the tetrabenzoporphyrin macrocycle. Importantly, orbitals in porphyrin **6** have well-defined parity, i.e., a_{2u} (HOMO) and b_{1u} (LUMO+2). Therefore, both the ground and the excited state (S_8) are the states of *g*-symmetry (A_g), which is a prerequisite for a high 2PA.

The strong stabilizing effect of the carbonyls is apparent in **6**: the energy of the 2P-accessible state (S_8) is shifted down significantly compared to the other studied molecules. Based on these calculations one should expect a substantial rise in 2PA above the B state, perhaps larger than in the case of **5**.

For *meso*-5,15-diaryltetrabenzoporphyrin **7** the situation is qualitatively similar. Two nearly degenerate excited states with strong 2PA character (S_8 and S_9) are stabilized to about the same level as in **6** (~3.5 eV), and their combined cross sections exceed 900 GM. The orbital configurations participating in the most 2P absorbing state (S_8) in **7** are similar to those in **6** (Figure S2). The target orbital (LUMO+4) is of b_{1u} symmetry, and therefore the 2P state is a *g*-symmetry state. In principle, the overlap between the laser spectrum and the absorption band encompassing states S_6–S_9 may even exceed that of **6**.

DOI: 10.1021/jacs.6b09157
J. Am. Chem. Soc. 2016, 138, 15648–15662

Table 3. Calculated and Experimental Data for Symmetric Pt Octaalkoxycarbonyl-tetrabenzoporphyrins[a,b]

	calculated				experimental						
compd no.	state	E singlets[c] (eV)	osc. strength[d]	$\sigma^{(2)}$ [e] (GM)	λ_{max} Q λ_{max} B (nm)	ε_{max} Q ε_{max} B (M^{-1} cm^{-1})	λ_{max}^{2P} [f] (nm)	$\sigma_{max}^{(2)}$ [g] (GM)	λ_{max} p[h] (nm)	ϕ_p [i]	τ [j] (μs)
6	S_1, S_2 (Q)	2.27, 2.27	0.47, 0.47	0.0, 0.0	605	184790	1150	11.4	743	0.45	58
	S_4, S_5 (B)	3.18, 3.18	1.56, 1.56	0.0, 0.0	415	199580					
	S_6, S_7	3.26, 3.26	0.0, 0.0	61.1, 19.9							
	S_8	3.49	0.0	789			800	503			
7	S_1, S_2 (Q)	2.25, 2.25	0.44, 0.43	0.0, 0.0	613	171570	1120	12.8	755	0.40	59
	S_3, S_4 (B)	3.10, 3.12	2.00, 1.41	0.0, 0.0	428	246600					
	S_6, S_7	3.24, 3.26	0.0, 0.0	26.1, 49.1							
	S_8, S_9	3.49, 3.50	0.0, 0.0	800, 117			850	89.7			

[a]For complete data sets see SI, p S20. [b]All measurements were performed in DMA and 22 °C. [c]Energies of singlet states S_n. Closely spaced states are grouped on the same line; only states relevant to the discussion are shown. [d]Oscillator strengths (for $S_0 \rightarrow S_n$). [e]2PA cross sections. [f]Excitation wavelengths at which the [g]maximal 2PA cross-section values in the Q and B state regions were observed. These table entries are shown in the same rows as the corresponding computed 2PA states (left-hand side). [h]"p" indicates phosphorescence. [i]ϕ_p is the phosphorescence quantum yield. [j]τ is the triplet lifetime.

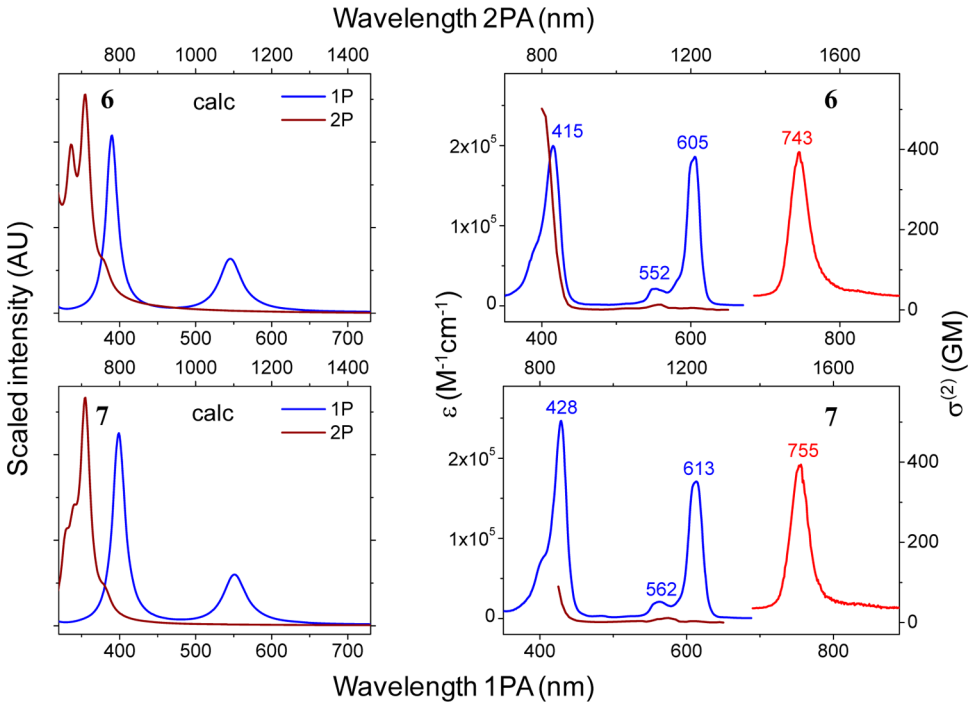

Figure 9. Calculated (left) and experimental (right) 1PA (blue), 2PA (brown), and phosphorescence (red) spectra of Pt octalkoxycarbonyl-substituted tetrabenzoporphyrins **6** and **7**. The vertical scales in the calculated spectra are the same.

However, we note that the linear absorption bands in **7** are red-shifted as a result of *meso*-aryl substitution, and by analogy with other porphyrins the phosphorescence band is shifted as well. Consequently, the lower lying triplet state may prevent excitation at the frequencies required to take the full advantage of the potentially strongly absorbing states S_6–S_9.

The experimental absorption and emission spectra and the photophysical data for porphyrins **6** and **7** are presented in Figure 9 and Table 3. The spectral lines in the calculated spectra were broadened by convolution with a Lorentzian function (Γ = 0.1 eV) to facilitate visual comparison with the experimental data.

We first note that despite giving higher absolute energies of the excited states, the calculations were able to predict trends in both 1PA and 2PA spectra remarkably well. There is indeed a dramatic enhancement in 2PA above the B state for *meso*-unsubstituted porphyrin **6** and a beginning of the rise in the case of **7**. That rise could not be followed because of the interfering linear $S_0 \rightarrow T_1$ absorption. The corresponding $\sigma^{(2)}{}_{max}$ values were found to be 503 and 89 GM for **6** and **7**, respectively. In the linear absorption spectra the effects of the substituents are also reproduced rather well, whereby the introduction of the *meso*-aryl groups in **7** leads to slight red shifts and a small change in the relative intensities of the B and Q transitions. Such good agreement between the experiment and theory significantly increases confidence in the ability of calculations to predict optical properties of these porphyrinoids.

DOI: 10.1021/jacs.6b09157
J. Am. Chem. Soc. 2016, 138, 15648–15662

Since porphyrins **6** and **7** possess nearly perfectly centrosymmetric structures, the observed enhancement of 2PA, as compared to either nonextended porphyrin **1** or benzo-unsubstituted porphyrin **4**, cannot be attributed to the change in the static dipole moments between the ground and final states (eq 4). At the same time, even for the shortest excitation wavelengths used in our experiments the detuning factors, i.e., the separation between the intermediate state (e.g., Q state) and the laser energy, were rather large, suggesting that the effect was not a consequence of the intermediate state resonance.[110] Instead, the dominant effect is again the stabilization of strongly 2P-allowed *g*-states, which involve alkoxycarbonyl groups and a conjugation pathway extending beyond the benzo-rings.

In view of the successful prediction of the optical spectra by calculations it was particularly interesting to examine how different excitation pathways, reflecting individual terms in the SOS expression, contribute to the overall 2PA. Tensor $\mathbf{S}^{(f)}$ (eq 3 and eq S5, p S18) can be represented by a matrix, whose diagonal elements $S_{00}^{(f)}$, $S_{11}^{(f)}$, ... $S_{NN}^{(f)}$ (N is the total number of states in the SOS expression) correspond to the pathways involving single intermediate state ψ_i: ($\psi_0 \rightarrow \psi_i \rightarrow \psi_f$). The off-diagonal elements can be viewed as mixed interference pathways,[107] which represent interacting pairs of transitions: ($\psi_0 \rightarrow \psi_i \rightarrow \psi_f | \psi_0 \rightarrow \psi_j \rightarrow \psi_f$).

A graphic representation of the matrix $\mathbf{S}^{(f)}$ for the strongly 2P-allowed transition in porphyrin **6** ($S_0 \rightarrow S_8$) is shown in Figure 10. The corresponding numerical values are given in

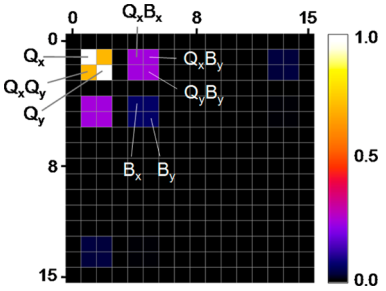

Figure 10. Color-coded matrix of the two-photon tensor $\mathbf{S}^{(f)}$ ($f = 8$) for 2P-allowed transition $S_0 \rightarrow S_8$ in porphyrin **6**. Only some pathways are labeled, while the other pathways are named in the text by analogy.

Table S1. In total 22 excited states were used in our calculations, however only 16 lowest states ($N = 0-15$) are shown. The contributions of higher lying states ($i > 15$) were found to be negligible. The scale in the image is normalized by the largest value in the matrix.

The largest contribution to the 2PA for state S_8 in **6** is indeed due to the Q state pathway(s): Q_x ($\psi_0 \rightarrow \psi_{Qx} \rightarrow \psi_f$), Q_y ($\psi_0 \rightarrow \psi_{Qy} \rightarrow \psi_f$), Q_xQ_y ($\psi_0 \rightarrow \psi_{Qx} \rightarrow \psi_f | \psi_0 \rightarrow \psi_{Qy} \rightarrow \psi_f$) and Q_yQ_x ($\psi_0 \rightarrow \psi_{Qy} \rightarrow \psi_f | \psi_0 \rightarrow \psi_{Qx} \rightarrow \psi_f$), qualitatively validating the three-state model. Nevertheless, even the pure B state pathway(s) (B_x, B_y, B_xB_y and B_yB_x) constitutes non-negligible ~8% of the Q pathway amplitude, which is in part due to the larger values of the transition dipole moments $\boldsymbol{\mu}_{B0}$ than $\boldsymbol{\mu}_{Q0}$: the corresponding oscillator strengths are $f_{B0} = 1.56$ and $f_{Q0} = 0.47$ for either *x*- or *y*-polarized transitions (Table 3). The larger detuning factor for the B pathway (1.43 eV) relative to that for the Q pathway (0.52 eV) along with a smaller transition dipole moment $\boldsymbol{\mu}_{fB}$ than $\boldsymbol{\mu}_{fQ}$ ($f_{fB} = 0.008$ vs $f_{fQ} = 0.13$) diminish the direct contribution of the B pathway. However, the mixed interference pathways (Q_xB_x, Q_xB_y, Q_yB_x and Q_yB_y) along with their conjugates (B_xQ_x, B_yQ_x, B_xQ_y, B_yQ_y) amount for >30% of the total transition amplitude, clearly illustrating the importance of the B state for 2PA in porphyrins.

One relevant detail emerging from this analysis is related to the transitions' polarizations. When using simplified models, such as the three-state model, it is commonly assumed that the transitions $\psi_0 \rightarrow \psi_Q$ and $\psi_Q \rightarrow \psi_f$ (Figure 1) are polarized parallel to one another.[102,107] Calculations show that this assumption may be incorrect. For example, in the case of porphyrin **6** transitions $\psi_0 \rightarrow \psi_{Qx}$ and $\psi_{Qx} \rightarrow \psi_f$ are polarized at an angle of ~50°, and the same is true for the pair $\psi_0 \rightarrow \psi_{Qy}$, $\psi_{Qy} \rightarrow \psi_f$ (SI, p S31).

Butoxycarbonyl groups in **7** vs **4** act virtually in the same way as in **5** vs **2** by inducing red shifts in the absorption spectra and lowering T_1-S_1 gap by ~0.05 eV, which is consistent with an increase in the size of the π-system due to the extended conjugation.[141] The phosphorescence quantum yields of both **6** and **7** are very high, placing both these porphyrins among the brightest existing triplet emitters.[55,84,145] A small decrease in the emissivity upon introduction of *meso*-aryl groups in **7** is a consequence of slight nonplanarity, paralleling measurements performed earlier on the analogous Pd porphyrins.[135] Compared to benzo-unsubstituted tetrabenzoporphyrin **4**, the phosphorescence quantum yield of **7** is almost twice as high, which is a result of a substantial increase in the triplet radiative decay rate constant upon introduction of the carbonyl substituents (Tables 1 and 3; SI, p S31). A similar effect was observed in **5** vs **2** (Table 1).

Lastly, it should be mentioned that both porphyrins **6** and **7** possess additional 2PA bands in the Q state region (SI, p S31), i.e., near 1100−1200 nm. Like in all other cases the absorption in the Q region is dominated by the vibronic bands Q_{10}, i.e., the smaller peaks shifted to the blue relative to the main Q_{00} transition. These bands are missing from our predictions, which did not include the vibronic contributions. Although the $\sigma^{(2)}$ values for these transitions do not exceed 10−15 GM, the possibility to excite far in the infrared may be attractive for deep tissue imaging applications.

CONCLUSIONS

The performed structure−property relationship study of a set of phosphorescent Pt(II) complexes of porphyrins in conjunction with electronic structure calculations made it possible to delineate effects of symmetry and peripheral substitution on their 1PA and 2PA absorption spectra and phosphorescence. The following conclusions can be drawn from this work:

(1) Fusion of the porphyrin macrocycle with external aromatic rings induces red shifts in the optical absorption spectra, but does not significantly affect the ability of Pt(II) porphyrins to phosphoresce. Their emission quantum yield remain high, i.e., ~0.4 for planar dibenzo- and tetrabenzoporphyrins, placing these porphyrins among the brightest triplet emitters known today.

(2) Lowering the symmetry of the macrocycle from D_{4h} to C_{2v} by way of *syn*-fusion with aromatic moieties leads to a moderate enhancement of 2PA into the 1P-allowed Q and B states.

(3) Addition of alkoxycarbonyl groups to the benzo-rings in *syn*-dibenzoporphyrin leads to a dramatic enhancement of 2PA in the B state region. The effect is due to the stabilization of 2P-active states, which are dominated by

DOI: 10.1021/jacs.6b09157
J. Am. Chem. Soc. 2016, 138, 15648−15662

configurations with orbitals extending onto the carbonyl groups.

(4) A similar yet larger effect is induced by alkoxycarbonyl groups in fully symmetric D_{4h} tetrabenzoporphyrins, where strongly 2P-active *g*-states are brought into the vicinity of the B state. The 2PA to these states is dominated by the Q state pathway ($\psi_0 \rightarrow \psi_Q \rightarrow \psi_f$), but in addition it is significantly enhanced by the quantum interference pathways mediated by the B state.

(5) Quantum-mechanical calculations based on the SOS formalism and TDDFT enable predictions of both 1P and 2P electronic absorption spectra of porphyrins, including aromatically π-extended porphyrins with substituents in benzo and/or *meso*-positions. These calculations make up a new useful tool, capable of aiding and directing experimental work on 2P porphyrinoids.

The key practical conclusion from this study is that Pt(II) complexes of aromatically π-extended carbonyl-substituted porphyrins make up a class of strongly 2P-absorbing chromophores with bright room-temperature phosphorescence. Unlike many other 2P-enhanced triplet molecules, these porphyrins are compact and relatively easy to synthesize, providing strong incentive to use them in relevant applications, especially when bright phosphorescence from the triplet states is required. On a more fundamental note, the mechanistic knowledge obtained through the studies of these model molecules should allow more efficient and better informed design of 2P chromophores as well as the analysis and evaluation of already existing structures.

■ ASSOCIATED CONTENT

Supporting Information

The Supporting Information is available free of charge on the ACS Publications website at DOI: 10.1021/jacs.6b09157.

Additional experimental details, optical spectroscopic data, and results of calculations, including Figures S1−S4 and Table S1 (PDF)

■ AUTHOR INFORMATION

Corresponding Author

*vinograd@mail.med.upenn.edu

ORCID

Sergei A. Vinogradov: 0000-0002-4649-5534

Notes

The authors declare no competing financial interest.

■ ACKNOWLEDGMENTS

Support by the grants EB018464, NS092986, and GM103591 from the National Institutes of Health, USA (S.A.V.), from the U.S. National Science Foundation through the Penn MRSEC DMR11-20901 and its optical microscopy SEF (S.A.V.), from the Swiss National Science Foundation (B.W.), from the Russian Science Foundation (contract no. 14-43-00052, operated by the Center of Photochemistry, Russian Academy of Sciences) and from Government of the Russian Federation Act 211, contract no. 02.A03.21.0011 (A.E.M.) is gratefully acknowledged. Computations were performed in part at the National Energy Research Scientific Computing Center (NERSC) and at the Advanced Research Computing Center (https://arcc.ist.ucf.edu) of the University of Central Florida. B.W. is a member of the Clinical Research Priority Program "Molecular Imaging Network Zurich". The authors are thankful to Dr. David Vann and Ms. Elizabeth Dempsey for assistance with ICP measurements.

■ REFERENCES

(1) Baldo, M. A.; O'Brien, D. F.; You, Y.; Shoustikov, A.; Sibley, S.; Thompson, M. E.; Forrest, S. R. *Nature* **1998**, *395*, 151.

(2) Borek, C.; Hanson, K.; Djurovich, P. I.; Thompson, M. E.; Aznavour, K.; Bau, R.; Sun, Y. R.; Forrest, S. R.; Brooks, J.; Michalski, L.; Brown, J. *Angew. Chem., Int. Ed.* **2007**, *46*, 1109.

(3) Perry, J. W.; Mansour, K.; Lee, I. S.; Wu, X.; Bedworth, P. V.; Chen, C. T.; Ng, D.; Marder, S. R.; Miles, P.; Wada, T.; Tian, M.; Sasabe, H. *Science* **1996**, *273*, 1533.

(4) Rogers, J. E.; Nguyen, K. A.; Hufnagle, D. C.; McLean, D. G.; Su, W. J.; Gossett, K. M.; Burke, A. R.; Vinogradov, S. A.; Pachter, R.; Fleitz, P. A. *J. Phys. Chem. A* **2003**, *107*, 11331.

(5) Monguzzi, A.; Bianchi, F.; Bianchi, A.; Mauri, M.; Simonutti, R.; Ruffo, R.; Tubino, R.; Meinardi, F. *Adv. Energy Mater.* **2013**, *3*, 680.

(6) Singh-Rachford, T. N.; Castellano, F. N. *Coord. Chem. Rev.* **2010**, *254*, 2560.

(7) Schulze, T. F.; Schmidt, T. W. *Energy Environ. Sci.* **2015**, *8*, 103.

(8) Srivatsan, A.; Missert, J. R.; Upadhyay, S. K.; Pandey, R. K. *J. Porphyrins Phthalocyanines* **2015**, *19*, 109.

(9) Abrahamse, H.; Hamblin, M. R. *Biochem. J.* **2016**, *473*, 347.

(10) Vanderkooi, J. M.; Maniara, G.; Green, T. J.; Wilson, D. F. *J. Biol. Chem.* **1987**, *262*, 5476.

(11) Vinogradov, S. A.; Wilson, D. F. In *Designing Dendrimers*; Capagna, S., Ceroni, P., Eds.; Wiley: New York, 2012.

(12) Quaranta, M.; Borisov, S. M.; Klimant, I. *Bioanal. Rev.* **2012**, *4*, 115.

(13) Papkovsky, D. B.; Dmitriev, R. I. *Chem. Soc. Rev.* **2013**, *42*, 8700.

(14) Goppert-Mayer, M. *Ann. Phys.* **2009**, *18*, 466.

(15) Theer, P.; Hasan, M. T.; Denk, W. *Opt. Lett.* **2003**, *28*, 1022.

(16) Shih, A. Y.; Driscoll, J. D.; Drew, P. J.; Nishimura, N.; Schaffer, C. B.; Kleinfeld, D. *J. Cereb. Blood Flow Metab.* **2012**, *32*, 1277.

(17) Oron, D.; Papagiakoumou, E.; Anselmi, F.; Emiliani, V. In *Optogenetics: Tools for Controlling and Monitoring Neuronal Activity*; Knopfel, T., Boyden, E. S., Eds.; Elsevier Science BV: Amsterdam, 2012; Vol. *196*, p 119.

(18) Wang, B. G.; Konig, K.; Halbhuber, K. J. *J. Microsc.* **2010**, *238*, 1.

(19) Denk, W.; Strickler, J. H.; Webb, W. W. *Science* **1990**, *248*, 73.

(20) Kerr, J. N. D.; Denk, W. *Nat. Rev. Neurosci.* **2008**, *9*, 195.

(21) Collins, H. A.; Khurana, M.; Moriyama, E. H.; Mariampillai, A.; Dahlstedt, E.; Balaz, M.; Kuimova, M. K.; Drobizhev, M.; Yang, V. X. D.; Phillips, D.; Rebane, A.; Wilson, B. C.; Anderson, H. L. *Nat. Photonics* **2008**, *2*, 420.

(22) Jeong, H. G.; Choi, M. S. *Isr. J. Chem.* **2016**, *56*, 110.

(23) Khurana, M.; Collins, H. A.; Karotki, A.; Anderson, H. L.; Cramb, D. T.; Wilson, B. C. *Photochem. Photobiol.* **2007**, *83*, 1441.

(24) Kim, K. S.; Lim, J. M.; Osuka, A.; Kim, D. *J. Photochem. Photobiol., C* **2008**, *9*, 13.

(25) Pawlicki, M.; Collins, H. A.; Denning, R. G.; Anderson, H. L. *Angew. Chem., Int. Ed.* **2009**, *48*, 3244.

(26) Aratani, N.; Kim, D.; Osuka, A. *Chem. - Asian J.* **2009**, *4*, 1172.

(27) Collini, E.; Mazzucato, S.; Zerbetto, M.; Ferrante, C.; Bozio, R.; Pizzotti, M.; Tessore, F.; Ugo, R. *Chem. Phys. Lett.* **2008**, *454*, 70.

(28) Morisue, M.; Ogawa, K.; Kamada, K.; Ohta, K.; Kobuke, Y. *Chem. Commun.* **2010**, *46*, 2121.

(29) Kamada, K.; Hara, C.; Ogawa, K.; Ohta, K.; Kobuke, Y. *Chem. Commun.* **2012**, *48*, 7988.

(30) Pawlicki, M.; Morisue, M.; Davis, N. K. S.; McLean, D. G.; Haley, J. E.; Beuerman, E.; Drobizhev, M.; Rebane, A.; Thompson, A. L.; Pascu, S. I.; Accorsi, G.; Armaroli, N.; Anderson, H. L. *Chem. Sci.* **2012**, *3*, 1541.

(31) Nowak-Krol, A.; Wilson, C. J.; Drobizhev, M.; Kondratuk, D. V.; Rebane, A.; Anderson, H. L.; Gryko, D. T. *ChemPhysChem* **2012**, *13*, 3966.

DOI: 10.1021/jacs.6b09157
J. Am. Chem. Soc. 2016, 138, 15648−15662

(32) Nowak-Krol, A.; Grzybowski, M.; Romiszewski, J.; Drobizhev, M.; Wicks, G.; Chotkowski, M.; Rebane, A.; Gorecka, E.; Gryko, D. T. *Chem. Commun.* **2013**, *49*, 8368.
(33) Mongin, O.; Sankar, M.; Charlot, M.; Mir, Y.; Blanchard-Desce, M. *Tetrahedron Lett.* **2013**, *54*, 6474.
(34) Wilkinson, J. D.; Wicks, G.; Nowak-Krol, A.; Lukasiewicz, L. G.; Wilson, C. J.; Drobizhev, M.; Rebane, A.; Gryko, D. T.; Anderson, H. L. *J. Mater. Chem. C* **2014**, *2*, 6802.
(35) Varnavski, O.; Raymond, J. E.; Yoon, Z. S.; Yotsutuji, T.; Ogawa, K.; Kobuke, Y.; Goodson, T., III. *J. Phys. Chem. C* **2014**, *118*, 28474.
(36) Schmitt, J.; Heitz, V.; Sour, A.; Bolze, F.; Ftouni, H.; Nicoud, J.-F.; Flamigni, L.; Ventura, B. *Angew. Chem., Int. Ed.* **2015**, *54*, 169.
(37) Mikhaylov, A.; Kondratuk, D. V.; Cnossen, A.; Anderson, H. L.; Drobizhev, M.; Rebane, A. *J. Phys. Chem. C* **2016**, *120*, 11663.
(38) Karotki, A.; Kruk, M.; Drobizhev, M.; Rebane, A.; Nickel, E.; Spangler, C. W. *IEEE J. Sel. Top. Quantum Electron.* **2001**, *7*, 971.
(39) Frederiksen, P. K.; McIlroy, S. P.; Nielsen, C. B.; Nikolajsen, L.; Skovsen, E.; Jorgensen, M.; Mikkelsen, K. V.; Ogilby, P. R. *J. Am. Chem. Soc.* **2005**, *127*, 255.
(40) Ogawa, K.; Kobuke, Y. *Anti-Cancer Agents Med. Chem.* **2008**, *8*, 269.
(41) Kuimova, M. K.; Collins, H. A.; Balaz, M.; Dahlstedt, E.; Levitt, J. A.; Sergent, N.; Suhling, K.; Drobizhev, M.; Makarov, N. S.; Rebane, A.; Anderson, H. L.; Phillips, D. *Org. Biomol. Chem.* **2009**, *7*, 889.
(42) Balaz, M.; Collins, H. A.; Dahlstedt, E.; Anderson, H. L. *Org. Biomol. Chem.* **2009**, *7*, 874.
(43) Hammerer, F.; Garcia, G.; Chen, S.; Poyer, F.; Achelle, S.; Fiorini-Debuisschert, C.; Teulade-Fichou, M. P.; Maillard, P. *J. Org. Chem.* **2014**, *79*, 1406.
(44) Finikova, O. S.; Lebedev, A. Y.; Aprelev, A.; Troxler, T.; Gao, F.; Garnacho, C.; Muro, S.; Hochstrasser, R. M.; Vinogradov, S. A. *ChemPhysChem* **2008**, *9*, 1673.
(45) Sakadzic, S.; Roussakis, E.; Yaseen, M. A.; Mandeville, E. T.; Srinivasan, V. J.; Arai, K.; Ruvinskaya, S.; Devor, A.; Lo, E. H.; Vinogradov, S. A.; Boas, D. A. *Nat. Methods* **2010**, *7*, 755.
(46) Lecoq, J.; Parpaleix, A.; Roussakis, E.; Ducros, M.; Houssen, Y. G.; Vinogradov, S. A.; Charpak, S. *Nat. Med.* **2011**, *17*, 893.
(47) Devor, A.; Sakadzic, S.; Saisan, P. A.; Yaseen, M. A.; Roussakis, E.; Srinivasan, V. J.; Vinogradov, S. A.; Rosen, B. R.; Buxton, R. B.; Dale, A. M.; Boas, D. A. *J. Neurosci.* **2011**, *31*, 13676.
(48) Parpaleix, A.; Houssen, Y. G.; Charpak, S. *Nat. Med.* **2013**, *19*, 241.
(49) Kazmi, S. M. S.; Salvaggio, A. J.; Estrada, A. D.; Hemati, M. A.; Shaydyuk, N. K.; Roussakis, E.; Jones, T. A.; Vinogradov, S. A.; Dunn, A. K. *Biomed. Opt. Express* **2013**, *4*, 1061.
(50) Spencer, J. A.; Ferraro, F.; Roussakis, E.; Klein, A.; Wu, J. W.; Runnels, J. M.; Zaher, W.; Mortensen, L. J.; Alt, C.; Turcotte, R.; Yusuf, R.; Cote, D.; Vinogradov, S. A.; Scadden, D. T.; Lin, C. P. *Nature* **2014**, *508*, 269.
(51) Lyons, D. G.; Parpaleix, A.; Roche, M.; Charpak, S. *eLife* **2016**, *5*, 12024.
(52) Kruk, M.; Karotki, A.; Drobizhev, M.; Kuzmitsky, V.; Gael, V.; Rebane, A. *J. Lumin.* **2003**, *105*, 45.
(53) Briñas, R. P.; Troxler, T.; Hochstrasser, R. M.; Vinogradov, S. A. *J. Am. Chem. Soc.* **2005**, *127*, 11851.
(54) Lebedev, A. Y.; Troxler, T.; Vinogradov, S. A. *J. Porphyrins Phthalocyanines* **2008**, *12*, 1261.
(55) Roussakis, E.; Spencer, J. A.; Lin, C.; Vinogradov, S. A. *Anal. Chem.* **2014**, *86*, 5937−5945.
(56) Wu, C. F.; Bull, B.; Christensen, K.; McNeill, J. *Angew. Chem., Int. Ed.* **2009**, *48*, 2741.
(57) Choi, N. W.; Verbridge, S. S.; Williams, R. M.; Chen, J.; Kim, J. Y.; Schmehl, R.; Farnum, C. E.; Zipfel, W. R.; Fischbach, C.; Stroock, A. D. *Biomaterials* **2012**, *33*, 2710.
(58) Lemon, C. M.; Karnas, E.; Han, X.; Bruns, O. T.; Kempa, T. J.; Fukumura, D.; Bawendi, M. G.; Jain, R. K.; Duda, D. G.; Nocera, D. G. *J. Am. Chem. Soc.* **2015**, *137*, 9832.
(59) Kondrashina, A.; Dmitriev, R.; Borisov, S.; Klimant, I.; Zhdanov, A.; Papkovsky, D. *FASEB J.* **2013**, *27*, 576.2.
(60) Dichtel, W. R.; Serin, J. M.; Edder, C.; Frechet, J. M. J.; Matuszewski, M.; Tan, L. S.; Ohulchanskyy, T. Y.; Prasad, P. N. *J. Am. Chem. Soc.* **2004**, *126*, 5380.
(61) Mongin, O.; Hugues, V.; Blanchard-Desce, M.; Merhi, A.; Drouet, S.; Yao, D.; Paul-Roth, C. *Chem. Phys. Lett.* **2015**, *625*, 151.
(62) Finikova, O. S.; Troxler, T.; Senes, A.; DeGrado, W. F.; Hochstrasser, R. M.; Vinogradov, S. A. *J. Phys. Chem. A* **2007**, *111*, 6977.
(63) Khan, A. A.; Fullerton-Shirey, S. K.; Howard, S. S. *RSC Adv.* **2015**, *5*, 291.
(64) Yoshihara, T.; Murayama, S.; Tobita, S. *Sensors* **2015**, *15*, 13503.
(65) Jana, A.; Crowston, B. J.; Shewring, J. R.; McKenzie, L. K.; Bryant, H. E.; Botchway, S. W.; Ward, A. D.; Amoroso, A. J.; Baggaley, E.; Ward, M. D. *Inorg. Chem.* **2016**, *55*, 5623.
(66) Gouterman, M. *J. Mol. Spectrosc.* **1961**, *6*, 138.
(67) Rubio-Pons, O.; Luo, Y.; Agren, H. *J. Chem. Phys.* **2006**, *124*, 094310.
(68) Jha, P. C.; Minaev, B.; Agren, H. *J. Chem. Phys.* **2008**, *128*, 074302.
(69) Morone, M.; Beverina, L.; Abbotto, A.; Silvestri, F.; Collini, E.; Ferrante, C.; Bozio, R.; Pagani, G. A. *Org. Lett.* **2006**, *8*, 2719.
(70) Esipova, T. V.; Vinogradov, S. A. *J. Org. Chem.* **2014**, *79*, 8812.
(71) Mikhailov, I. A.; Tafur, S.; Masunov, A. E. *Phys. Rev. A: At., Mol., Opt. Phys.* **2008**, *77*, 012510.
(72) Mikhailov, I. A.; Musial, M.; Masunov, A. E. *Comput. Theor. Chem.* **2013**, *1019*, 23.
(73) Nayyar, I. H.; Masunov, A. E.; Tretiak, S. *J. Phys. Chem. C* **2013**, *117*, 18170.
(74) Mikhailov, I. A.; Belfield, K. D.; Masunov, A. E. *J. Phys. Chem. A* **2009**, *113*, 7080.
(75) Belfield, K. D.; Bondar, M. V.; Hernandez, F. E.; Masunov, A. E.; Mikhailov, I. A.; Morales, A. R.; Przhonska, O. V.; Yao, S. *J. Phys. Chem. C* **2009**, *113*, 4706.
(76) Toro, C.; De Boni, L.; Yao, S.; Ritchie, J. P.; Masunov, A. E.; Belfield, K. D.; Hernandez, F. E. *J. Chem. Phys.* **2009**, *130*, 214504.
(77) Masunov, A. E.; Mikhailov, I. A. *Eur. J. Chem.* **2010**, *1*, 142.
(78) Belfield, K. D.; Bondar, M. V.; Frazer, A.; Morales, A. R.; Kachkovsky, O. D.; Mikhailov, I. A.; Masunov, A. E.; Przhonska, O. V. *J. Phys. Chem. B* **2010**, *114*, 9313.
(79) Webster, S.; Peceli, D.; Hu, H.; Padilha, L. A.; Przhonska, O. V.; Masunov, A. E.; Gerasov, A. O.; Kachkovski, A. D.; Slominsky, Y. L.; Tolmachev, A. I.; Kurdyukov, V. V.; Viniychuk, O. O.; Barrasso, E.; Lepkowicz, R.; Hagan, D. J.; Van Stryland, E. W. *J. Phys. Chem. Lett.* **2010**, *1*, 2354.
(80) Luchita, G.; Bondar, M. V.; Yao, S.; Mikhailov, I. A.; Yanez, C. O.; Przhonska, O. V.; Masunov, A. E.; Belfield, K. D. *ACS Appl. Mater. Interfaces* **2011**, *3*, 3559.
(81) Moreshead, W. V.; Przhonska, O. V.; Bondar, M. V.; Kachkovski, A. D.; Nayyar, I. H.; Masunov, A. E.; Woodward, A. W.; Belfield, K. D. *J. Phys. Chem. C* **2013**, *117*, 23133.
(82) Peceli, D.; Hu, H.; Fishman, D. A.; Webster, S.; Przhonska, O. V.; Kurdyukov, V. V.; Slominsky, Y. L.; Tolmachev, A. I.; Kachkovski, A. D.; Gerasov, A. O.; Masunov, A. E.; Hagan, D. J.; Van Stryland, E. W. *J. Phys. Chem. A* **2013**, *117*, 2333.
(83) Croitor, L.; Coropceanu, E. B.; Masunov, A. E.; Rivera-Jacquez, H. J.; Siminel, A. V.; Fonari, M. S. *J. Phys. Chem. C* **2014**, *118*, 9217.
(84) Finikova, O. S.; Cheprakov, A. V.; Vinogradov, S. A. *J. Org. Chem.* **2005**, *70*, 9562.
(85) Filatov, M. A.; Lebedev, A. Y.; Vinogradov, S. A.; Cheprakov, A. V. *J. Org. Chem.* **2008**, *73*, 4175.
(86) Kubin, R. F.; Fletcher, A. N. *J. Lumin.* **1982**, *27*, 455.
(87) Finikova, O. S.; Aleshchenkov, S. E.; Brinas, R. P.; Cheprakov, A. V.; Carroll, P. J.; Vinogradov, S. A. *J. Org. Chem.* **2005**, *70*, 4617.
(88) Xu, C.; Webb, W. W. *J. Opt. Soc. Am. B* **1996**, *13*, 481.
(89) Makarov, N. S.; Drobizhev, M.; Rebane, A. *Opt. Express* **2008**, *16*, 4029.
(90) Frisch, M. J.; Trucks, G. W.; Schlegel, H. B.; Scuseria, G. E.; Robb, M. A.; Cheeseman, J. R.; Scalmani, G.; Barone, V.; Mennucci, B.; Petersson, G. A.; Nakatsuji, H.; Caricato, M.; Li, X.; Hratchian, H.

DOI: 10.1021/jacs.6b09157
J. Am. Chem. Soc. 2016, 138, 15648−15662

P.; Izmaylov, A. F.; Bloino, J.; Zheng, G.; Sonnenberg, J. L.; Hada, M.; Ehara, M.; Toyota, K.; Fukuda, R.; Hasegawa, J.; Ishida, M.; Nakajima, T.; Honda, Y.; Kitao, O.; Nakai, H.; Vreven, T.; Montgomery, J. A., Jr.; Peralta, J. E.; Ogliaro, F.; Bearpark, M.; Heyd, J. J.; Brothers, E.; Kudin, K. N.; Staroverov, V. N.; Kobayashi, R.; Normand, J.; Raghavachari, K.; Rendell, A.; Burant, J. C.; Iyengar, S. S.; Tomasi, J.; Cossi, M.; Rega, N.; Millam, N. J.; Klene, M.; Knox, J. E.; Cross, J. B.; Bakken, V.; Adamo, C.; Jaramillo, J.; Gomperts, R.; Stratmann, R. E.; Yazyev, O.; Austin, A. J.; Cammi, R.; Pomelli, C.; Ochterski, J. W.; Martin, R. L.; Morokuma, K.; Zakrzewski, V. G.; Voth, G. A.; Salvador, P.; Dannenberg, J. J.; Dapprich, S.; Daniels, A. D.; Farkas, Ö.; Foresman, J. B.; Ortiz, J. V.; Cioslowski, J.; Fox, D. J. *Gaussian 09*; Gaussian, Inc.: Wallingford, CT, 2009.

(91) Mikhailov, I. A.; Bondar, M. V.; Belfield, K. D.; Masunov, A. E. *J. Phys. Chem. C* **2009**, *113*, 20719.

(92) Zhao, Y.; Schultz, N. E.; Truhlar, D. G. *J. Chem. Theory Comput.* **2006**, *2*, 364.

(93) Andrae, D.; Haussermann, U.; Dolg, M.; Stoll, H.; Preuss, H. *Theor. Chim. Acta* **1990**, *77*, 123.

(94) Dunning, T. H., Jr.; Hay, P. J. In *Methods of Electronic Structure Theory*; Schaefer, H. F., III, Ed.; Springer: New York, 1977; Vol. 3, p 1.

(95) Masunov, A. E. M.; Mikhailov, I. A. *Eur. J. Chem.* **2010**, *1*, 142.

(96) Marenich, A. V.; Cramer, C. J.; Truhlar, D. G. *J. Phys. Chem. B* **2009**, *113*, 6378.

(97) Ohta, K.; Kamada, K. *J. Chem. Phys.* **2006**, *124*, 124303.

(98) Tretiak, S.; Mukamel, S. *Chem. Rev.* **2002**, *102*, 3171.

(99) Chernyak, V.; Mukamel, S. *J. Chem. Phys.* **2000**, *112*, 3572.

(100) Mikhailov, I. A.; Tafur, S.; Masunov, A. E. *Phys. Rev. A: At., Mol., Opt. Phys.* **2008**, *77*, 012510.

(101) Masthay, M. B.; Findsen, L. A.; Pierce, B. M.; Bocian, D. F.; Lindsey, J. S.; Birge, R. R. *J. Chem. Phys.* **1986**, *84*, 3901.

(102) Karotki, A.; Drobizhev, M.; Kruk, M.; Spangler, C.; Nickel, E.; Mamardashvili, N.; Rebane, A. *J. Opt. Soc. Am. B* **2003**, *20*, 321.

(103) Ohira, S.; Bredas, J. L. *J. Mater. Chem.* **2009**, *19*, 7545.

(104) Day, P. N.; Nguyen, K. A.; Pachter, R. *J. Chem. Theory Comput.* **2008**, *4*, 1094.

(105) Greco, J. A.; Shima, S.; Wagner, N. L.; McCarthy, J. R.; Atticks, K.; Brueckner, C.; Birge, R. R. *J. Phys. Chem. C* **2015**, *119*, 3711.

(106) Alam, M. M.; Daniel, C. *Theor. Chem. Acc.* **2016**, DOI: 10.1007/s00214-015-1780-x.

(107) Drobizhev, M.; Meng, F. Q.; Rebane, A.; Stepanenko, Y.; Nickel, E.; Spangler, C. W. *J. Phys. Chem. B* **2006**, *110*, 9802.

(108) Makarov, N. S.; Drobizhev, M.; Wicks, G.; Makarova, E. A.; Lukyanets, E. A.; Rebane, A. *J. Chem. Phys.* **2013**, *138*, 214314.

(109) Drobizhev, M.; Karotki, A.; Kruk, M.; Mamardashvili, N. Z.; Rebane, A. *Chem. Phys. Lett.* **2002**, *361*, 504.

(110) Drobizhev, M.; Karotki, A.; Kruk, M.; Rebane, A. *Chem. Phys. Lett.* **2002**, *355*, 175.

(111) Drobizhev, M.; Stepanenko, Y.; Dzenis, Y.; Karotki, A.; Rebane, A.; Taylor, P. N.; Anderson, H. L. *J. Am. Chem. Soc.* **2004**, *126*, 15352.

(112) Drobizhev, M.; Stepanenko, Y.; Dzenis, Y.; Karotki, A.; Rebane, A.; Taylor, P. N.; Anderson, H. L. *J. Phys. Chem. B* **2005**, *109*, 7223.

(113) Drobizhev, M.; Stepanenko, Y.; Rebane, A.; Wilson, C. J.; Screen, T. E. O.; Anderson, H. L. *J. Am. Chem. Soc.* **2006**, *128*, 12432.

(114) Rumi, M.; Barlow, S.; Wang, J.; Perry, J. W.; Marder, S. R. In *Photoresponsive Polymers I*; Marder, S. R., Lee, K. S., Eds.; Springer: Berlin, 2008; Vol. *213*, p 1.

(115) Terenziani, F.; Katan, C.; Badaeva, E.; Tretiak, S.; Blanchard-Desce, M. *Adv. Mater.* **2008**, *20*, 4641.

(116) McClain, W. M. *Acc. Chem. Res.* **1974**, *7*, 129.

(117) Birge, R. R.; Pierce, B. M. *J. Chem. Phys.* **1979**, *70*, 165.

(118) Boyd, R. W.*Non-linear optics*; Elsevier Inc.: Oxford, UK, 2008.

(119) Monson, P. R.; McClain, W. M. *J. Chem. Phys.* **1970**, *53*, 29.

(120) Monson, P. R.; McClain, W. M. *J. Chem. Phys.* **1972**, *56*, 4817.

(121) Luo, Y.; Rubio-Pons, O.; Guo, J. D.; Agren, H. *J. Chem. Phys.* **2005**, *122*, 096101.

(122) Casida, M. E.; Jamorski, C.; Casida, K. C.; Salahub, D. R. *J. Chem. Phys.* **1998**, *108*, 4439.

(123) Hu, H. H.; Fishman, D. A.; Gerasov, A. O.; Przhonska, O. V.; Webster, S.; Padilha, L. A.; Peceli, D.; Shandura, M.; Kovtun, Y. P.; Kachkovski, A. D.; Nayyar, I. H.; Masunov, A. E.; Tongwa, P.; Timofeeva, T. V.; Hagan, D. J.; Van Stryland, E. W. *J. Phys. Chem. Lett.* **2012**, *3*, 1222.

(124) Gouterman, M. *J. Chem. Phys.* **1959**, *30*, 1139.

(125) Thorne, J. R. G.; Kuebler, S. M.; Denning, R. G.; Blake, I. M.; Taylor, P. N.; Anderson, H. L. *Chem. Phys.* **1999**, *248*, 181.

(126) Karotki, A.; Drobizhev, M.; Dzenis, Y.; Taylor, P. N.; Anderson, H. L.; Rebane, A. *Phys. Chem. Chem. Phys.* **2004**, *6*, 7.

(127) Luo, Y.; Rubio-Pons, O.; Guo, J.-D.; Ågren, H. *J. Chem. Phys.* **2005**, *122*, 096101.

(128) Knyukshto, V. N.; Shul'ga, A. M.; Sagun, E. I.; Zen'kevich, E. I. *Opt. Spectrosc.* **2006**, *100*, 590.

(129) Kobayashi, T.; Straub, K. D.; Rentzepis, P. M. *Photochem. Photobiol.* **1979**, *29*, 925.

(130) Eastwood, D.; Gouterman, M. *J. Mol. Spectrosc.* **1970**, *35*, 359.

(131) Magde, D.; Windsor, M. W.; Holten, D.; Gouterman, M. *Chem. Phys. Lett.* **1974**, *29*, 183.

(132) Wurth, C.; Grabolle, M.; Pauli, J.; Spieles, M.; Resch-Genger, U. *Nat. Protoc.* **2013**, *8*, 1535.

(133) Kobayashi, N.; Konami, H. *J. Porphyrins Phthalocyanines* **2001**, *5*, 233.

(134) Rosa, A.; Ricciardi, G.; Baerends, E. J.; van Gisbergen, S. J. A. *J. Phys. Chem. A* **2001**, *105*, 3311.

(135) Lebedev, A. Y.; Filatov, M. A.; Cheprakov, A. V.; Vinogradov, S. A. *J. Phys. Chem. A* **2008**, *112*, 7723.

(136) Sommer, J. R.; Shelton, A. H.; Parthasarathy, A.; Ghiviriga, I.; Reynolds, J. R.; Schanze, K. S. *Chem. Mater.* **2011**, *23*, 5296.

(137) Kim, P.; Sung, J.; Uoyama, H.; Okujima, T.; Uno, H.; Kim, D. *J. Phys. Chem. B* **2011**, *115*, 3784.

(138) Rosa, A.; Ricciardi, G.; Baerends, E. J. *J. Phys. Chem. A* **2006**, *110*, 5180.

(139) Gentemann, S.; Medforth, C. J.; Forsyth, T. P.; Nurco, D. J.; Smith, K. M.; Fajer, J.; Holten, D. *J. Am. Chem. Soc.* **1994**, *116*, 7363.

(140) Gentemann, S.; Nelson, N. Y.; Jaquinod, L.; Nurco, D. J.; Leung, S. H.; Medforth, C. J.; Smith, K. M.; Fajer, J.; Holten, D. *J. Phys. Chem. B* **1997**, *101*, 1247.

(141) McGlynn, S. P.; Azumi, T.; Kinoshita, M.*Molecular spectroscopy of the triplet state*; Prentice-Hall: Englewood Cliffs, NJ, 1969.

(142) Lebedev, A. Y.; Cheprakov, A. V.; Sakadzic, S.; Boas, D. A.; Wilson, D. F.; Vinogradov, S. A. *ACS Appl. Mater. Interfaces* **2009**, *1*, 1292.

(143) Ito, S.; Murashima, T.; Uno, H.; Ono, N. *Chem. Commun.* **1998**, 1661.

(144) Finikova, O.; Cheprakov, A.; Beletskaya, I.; Vinogradov, S. *Chem. Commun.* **2001**, 261.

(145) Roussakis, E.; Li, Z. X.; Nowell, N. H.; Nichols, A. J.; Evans, C. L. *Angew. Chem., Int. Ed.* **2015**, *54*, 14728.

DOI: 10.1021/jacs.6b09157
J. Am. Chem. Soc. 2016, 138, 15648−15662